Static and Dynamic Factors Limit Chromosomal Replication Complexity in *Escherichia coli*, Avoiding Dangers of Runaway Overreplication

Sharik R. Khan, Tulip Mahaseth, Elena A. Kouzminova, Glen E. Cronan, and Andrei Kuzminov[1]
Department of Microbiology, University of Illinois at Urbana-Champaign, Urbana, Illinois 61801

ABSTRACT We define chromosomal replication complexity (CRC) as the ratio of the copy number of the most replicated regions to that of unreplicated regions on the same chromosome. Although a typical CRC of eukaryotic or bacterial chromosomes is 2, rapidly growing *Escherichia coli* cells induce an extra round of replication in their chromosomes (CRC = 4). There are also *E. coli* mutants with stable CRC∼6. We have investigated the limits and consequences of elevated CRC in *E. coli* and found three limits: the "natural" CRC limit of ∼8 (cells divide more slowly); the "functional" CRC limit of ∼22 (cells divide extremely slowly); and the "tolerance" CRC limit of ∼64 (cells stop dividing). While the natural limit is likely maintained by the eclipse system spacing replication initiations, the functional limit might reflect the capacity of the chromosome segregation system, rather than dedicated mechanisms, and the tolerance limit may result from titration of limiting replication factors. Whereas recombinational repair is beneficial for cells at the natural and functional CRC limits, we show that it becomes detrimental at the tolerance CRC limit, suggesting recombinational misrepair during the runaway overreplication and giving a rationale for avoidance of the latter.

KEYWORDS overinitiation; hydroxyurea; *seqA*; *rep*; *recA*

EUKARYOTIC and prokaryotic chromosomes differ in many important aspects (Kuzminov 2014), and one key difference lies in the spatio-temporal organization of chromosomal replication. In contrast to eukaryotes, which perform multibubble replication (Masai *et al.* 2010), most bacteria replicate their singular chromosome in the unibubble format by initiating bidirectional replication from a designated replication origin (*oriC*) (Sernova and Gelfand 2008; Leonard and Méchali 2013) and finishing replication within a broad termination zone (*ter*) (Mirkin and Mirkin 2007; Duggin *et al.* 2008). Eukaryotes always perform a single replication round in their chromosomes (Masai *et al.* 2010; Diffley 2011), keeping the ratio of maximally replicated to unreplicated DNA in the same chromosome (the "replication complexity index") strictly at 2 (Figure 1A). Due to the defined origin and terminus of prokaryotic chromosomes, chromosomal replication complexity in bacteria can be simply expressed as the ori/ter ratio (Figure 1B). Even though unique cell cycles in some bacteria, such as *Caulobacter*, also maintain a strict CRC = 2 (Collier 2012), bacterial cells are generally recognized for their ability to support multiple concurrent replication rounds within the same chromosome (Morigen *et al.* 2009).

In reality, under typical growth conditions the ori/ter ratio in exponentially growing bacterial cells is still ∼2 (Bird *et al.* 1972; Bipatnath *et al.* 1998; Wang *et al.* 2007; Murray and Errington 2008; Rotman *et al.* 2009; Stokke *et al.* 2011), showing that bacterial cells, like eukaryotes, also prefer to deal with a single replication round in their chromosomes. However, due to the peculiarity of the prokaryotic chromosome cycle (Kuzminov 2013), when the rate of cell mass duplication surpasses the genome duplication rate [*Escherichia coli* cannot replicate its chromosome in less than ∼40 min (Chandler *et al.* 1975; Bremer and Dennis 1996)], *E. coli* and some other bacteria are capable of initiating additional replication rounds in the same chromosome. For example, *E. coli* cells dividing every 20 min double their chromosomal replication complexity (ori/ter) to ∼4 (Morigen *et al.* 2009), a state referred to as "multifork replication" (Cooper and Helmstetter 1968; Quinn and Sueoka 1970) (Figure 1B).

doi: 10.1534/genetics.115.184697
Manuscript received November 10, 2015; accepted for publication January 17, 2016; published Early Online January 21, 2016.
Supporting information is available online at www.genetics.org/lookup/suppl/doi:10.1534/genetics.115.184697/-/DC1.
[1]Corresponding author: University of Illinois at Urbana-Champaign, B103 C&LSL, 601 South Goodwin Ave., Urbana, IL 61801-3709. E-mail: kuzminov@life.illinois.edu

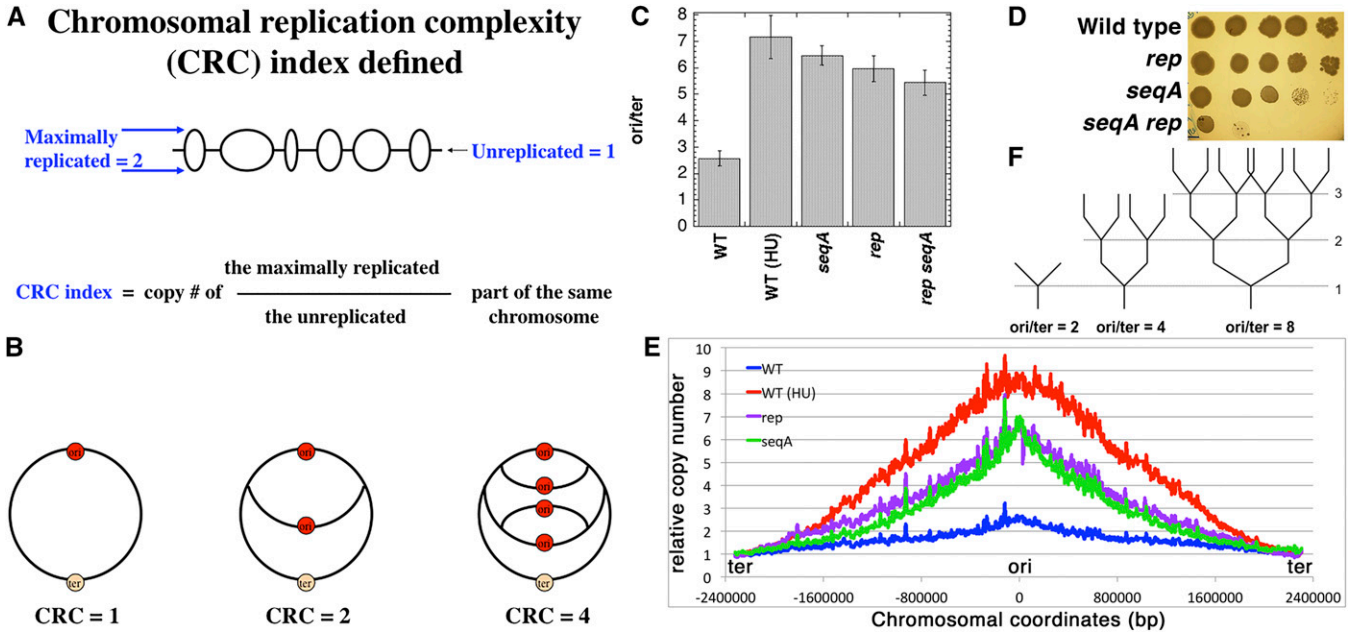

Figure 1 Increased replication complexity in cells with slow replication forks reveals the "natural" CRC limit. All cultures in Figure 1 and Figure 2 were grown at 28°; thus, the wild-type doubling time is ~40 min, and the ori/ter ratio is ~2. (A) A scheme of the replicating eukaryotic chromosome and the definition of the CRC index. (B) The replication complexity of the bacterial chromosome is simply expressed (and measured) as the origin-to-terminus ratio. (C) Ori/ter ratios in growing *E. coli* cultures of the indicated mutants (or conditions). (D) Serial dilutions of growing cultures with the corresponding genotypes were spotted to illustrate growth rate differences. (E) Chromosomal marker-frequency profiles of the growing cultures of wild-type, wild-type (HU), *rep*, and *seqA* strains. (F) Schematic chromosomal replication complexity at various ori/ter ratios. The chromosomes are shown as lines, and the replication points as Y-junctions. The chromosomes at different replication complexities are not to scale to align the replication points (numbered on the right).

Is multifork replication observed only in the fastest-growing bacterial cells? In fact, even with a modest rate of cell mass increase, inhibition of replication fork progression will cause bacterial cells to employ multi-fork replication. A classic condition in bacteria when the DNA replication rate lags behind that of cell mass accumulation is thymine limitation (when the limited availability of the DNA precursors dTTP reduces the replication rate) (Ahmad *et al.* 1998). Thymine-limited *E. coli* cells have 100% viability, show normal growth rates, and divide on time, but their CRC increases to compensate for the slower-moving replication forks (Zaritsky *et al.* 2006). The system that regulates these extra initiations is proposed to be the one that determines the "eclipse period," a cell cycle phase of enforced origin inactivity following each replication initiation, lasting ~60% of the generation time (von Freiesleben *et al.* 2000; Olsson *et al.* 2002). By preventing closely spaced origin firing events, the eclipse phenomenon defines a minimal allowed distance between codirectional replication forks in the *E. coli* chromosome.

Theoretical considerations of the eclipse phenomenon predicted a natural upper limit for increased chromosomal replication complexity in *E. coli* replicating under conditions of thymine limitation of two replication rounds per chromosome (CRC = 4, Figure 1B) before accumulation of inhibitory chromosomal problems of unknown nature (Zaritsky *et al.* 2006, 2007). For example, initiation from multiple origins in the same cell becomes asynchronous when the eclipse period is reduced below half-a-generation time (Olsson *et al.* 2003). Indeed, maximal reported ori/ter values in thymine-limited cells generally do not go over 4 (Bird *et al.* 1972; Martín and Guzmán 2011; Kuong and Kuzminov 2012), and when they are forced to cross this barrier by acute thymine starvation (which causes massive cell die-off called "thymineless death"), chromosomes do suffer catastrophic loss of the origin macrodomain, the causes of which remain unclear (Sangurdekar *et al.* 2010; Kuong and Kuzminov 2012). In *Vibrio cholera* and *Bacillus subtilis*, also capable of more than one replication round per chromosome, the maximal reported ori/ter ratio is also 4 (Wang *et al.* 2007; Stokke *et al.* 2011). All these observations are consistent with existence of a "hard" natural CRC limit at two rounds per chromosome, enforced by the poorly understood eclipse phenomenon.

The existence of the natural CRC = 4 limit is challenged, however, in some mutants of *E. coli* or in wild-type cells grown under certain conditions. The *hda* mutants that possess a defective negative regulator of replication initiation have an ori/ter ratio close to 5 (Morigen *et al.* 2009). A defect in nucleotide reductase, the enzyme that supplies replication forks with DNA precursors, also increases the ori/ter ratio to 5 (Salguero *et al.* 2011). A nucleotide reductase inhibitor, hydroxyurea (HU), reduces DNA replication rate in *E. coli* to 20% of the uninhibited rate (Kuong and Kuzminov 2009) and, within 4 hr, brings the ori/ter ratio to ~5 (Kuong and Kuzminov 2012). Mutants in the *rep* have gene slow

replication forks due to the absence of an auxiliary replicative helicase (Atkinson *et al.* 2011) and display an apparent ori/ter ratio of ~6 (Lane and Denhardt 1975).

Perhaps the highest known steady-state ori/ter ratio of ~6.5 is reported in the slow-growing *seqA* mutants, deficient in another negative regulator of replication initiation independent of Hda above (Rotman *et al.* 2009, 2014). SeqA protein binds to hemi-methylated *oriC* DNA, blocking DnaA polymerization over it and thus preventing premature initiation (reviewed in Waldminghaus and Skarstad 2009). Eventually, all the multiple GATC sites in *oriC* are fully methylated by the Dam methyltransferase, resulting in SeqA/*oriC* disassociation and making *oriC* initiation-proficient again (initiation itself may not happen for another hour due to operation of other regulatory circuits) (reviewed in Skarstad and Katayama 2013). In the *seqA* mutants, initiations are less regulated and also less synchronized compared to SeqA+ cells, leading to initial overinitiation in rapidly growing cells (Rotman *et al.* 2014). However, the subsequent initiations in *seqA* mutants are not runaway (uncontrolled) in nature, presumably due to slowing down of replication forks (the actual reason is still unknown) (Rotman *et al.* 2014). Interestingly, in *seqA* mutants the eclipse period is reduced to a bare minimum—as if it were determined by segregation itself—suggesting that origin sequestration by SeqA is the major eclipse factor (Olsson *et al.* 2002, 2003).

In contrast to thymineless death (Sangurdekar *et al.* 2010; Kuong and Kuzminov 2012), cells subjected to other conditions known to cause replication fork inhibition incur no known irreparable chromosomal damage (the mutants with elevated ori/ter ratio do grow more slowly), showing that elevated CRC = 6 can be safely handled and causes neither cell death nor inhibition of the cell cycle. Perhaps thymine starvation is an exception to its sensitivity to increased CRC, while the eclipse phenomenon can be thought of as merely a time measure that standardizes distance between consecutive replication forks when fork progression is slowed, as in *seqA* mutants (Olsson *et al.* 2002). On the other hand, *E. coli* mutants with increased CRC suffer from increased chromosomal fragmentation (Michel *et al.* 1997; Rotman *et al.* 2014), while in humans increased CRC is linked to chromosome rearrangements (Hastings *et al.* 2009; Zhang *et al.* 2009) and carcinogenesis (Hook *et al.* 2007; Truong *et al.* 2014), suggesting that increased CRC is an important factor of genome instability.

The initial objectives of this study were, by pushing *E. coli* cells to maximize chromosomal replication complexity (in the *rep* and *seqA* mutants or in HU-treated cells): (1) to confirm the maximal chromosomal replication complexity that *E. coli* can routinely achieve without major adverse consequences—the natural CRC limit; (2) to determine the maximal chromosomal replication complexity at which *E. coli* can still slowly grow—the functional CRC limit; (3) to push *E. coli* to develop the maximal chromosomal replication complexity that the cells can survive—the tolerance CRC limit; (4) to understand the nature of growth inhibition due to the increased CRC. In our efforts to maximize CRC, we specifically avoided the subject of regulation of the replication initiation at the chromosomal origin and, in fact, removed this consideration altogether in subsequent experimentation by initiating chromosome replication from an inducible plasmid replication origin.

Materials and Methods

Bacterial strains and growth conditions

All strains used in this study are derivatives of *E. coli* strain K12 and are described in Supporting Information, Table S1. Strains were grown with shaking in LB [10 g of tryptone, 5 g of yeast extract, 5 g of NaCl, 250 μl of 4 M NaOH per liter (Miller 1972)] supplemented with appropriate antibiotics: ampicillin, 100 μg/ml; spectinomycin, 100 μg/ml; kanamycin, 50 μg/ml; chloramphenicol, 10 μg/ml; and tetracycline, 10 μg/ml. Growth in liquid cultures was with vigorous shaking, typically at 28°, but, in all experiments with IPTG induction (1 mM), the temperature was 37°. Genetic alterations were made by λ Red-promoted gene replacement (Datsenko and Wanner 2000). Alleles were moved among the strains by P1 transduction (Miller 1972). DNA repair mutants were confirmed by characteristic UV sensitivities, as well as physically, by either Southern hybridization or by PCR. The *seqA* mutants were confirmed by their sensitivity to low temperatures (22°), to 1% SDS or to 1 mM hydroxyurea.

Plasmids

Plasmid pAM34 has been described before (Gil and Bouché 1991). A derivative of pAM34 containing bidirectionally oriented inducible origins was generated in multiple steps. In the first step, pAM34 was digested with *Bal*I and *Pst*I, and the 1928-bp fragment containing inducible origin with its regulatory elements was gel-purified (fragment I). In the second step, pAM34 was digested with *Pst*I and *Sma*I, resulting in the excision of a 1657-bp fragment containing the *ada* gene. From this digestion, the 4343-bp fragment containing inducible origin, *bla*, and *lacI* was gel-purified (fragment 2). In the third step, a 2091-bp fragment (genomic coordinates 3,929,116–3,931,207) containing the *kup* locus was PCR-amplified using oligonucleotides harboring *Pst*I sites. This fragment was purified, digested with *Pst*I, and repurified (fragment 3). The three fragments were ligated, transformed into AB1157, and plated onto LB plates containing ampicillin and IPTG. Several ampicillin-resistant transformants were screened for spectinomycin sensitivity and tested by restriction digestion. One ~8.3-kb construct containing a copy of the *kup* gene flanked by two oppositely oriented copies of inducible origins was named "pSRK-ori2" and used further.

Construction of inducible, bidirectional origin strain

Plasmid pSRK-ori2, which harbors chromosomal homology to the *kup* locus, was used as a conditional vector to create extra origin constructs (Figure S3). For the genomic integration of

plasmid at the *kup* locus, overnight culture of AB1157 (pSRK-ori2) grown in the presence of IPTG was serially diluted and plated onto LB agar without IPTG. The ampicillin-resistant colonies obtained in the absence of IPTG were streaked for isolation, and one candidate, 1157-Inducible Origin Construct (IOC), was chosen for studies. Tranformation and integration of plasmid pSRK-ori2 into SK129 resulted in the generation of strain SRK325 [*recBC*(Ts)-IOC], which has been used previously (Rotman *et al.* 2014).

Creation of IOC strains resulted in the duplication of *kup* locus, making the plasmid integration potentially unstable, especially when the strains were grown in the presence of IPTG. While we did not see any replicating plasmid when IOC strains were grown in presence of IPTG, we stabilized SRK325 [*recBC*(Ts)-IOC] by replacing one copy of *kup* locus with a kanamycin cassette of pKD4 (Datsenko and Wanner 2000). The resulting strain, SRK252 [*recBC*(Ts)-IOC::*kan*], was screened by PCR for the loss of the copy of the *kup* locus and incorporation of the kanamycin cassette. The inducible stable origins from strain SRK252 were moved into AB1157 by P1 transduction, generating strain SRK253 (AB1157-IOC::*kan*). Additional mutations in SRK252 and SRK253 were introduced by P1 transduction as described in Table S1.

Viability assays

Strains were inoculated in LB medium containing appropriate antibiotics at 28°. Following overnight growth, the cultures were diluted 20×–100× in fresh LB medium and incubated with shaking at 37° until A_{600} = 0.2. At this time, the titer of the culture was measured, and one-half of the culture was induced with 1 mM IPTG. Both induced and un-induced cultures were further incubated at the appropriate temperatures and periodically titered (serially diluted in sterile 1% NaCl and spotted by 10 μl onto freshly made duplicate LB plates). The plates were incubated at 37°, and colonies were counted under the microscope while they were still a pin prick in size.

Acute HU treatment

AB1157, *seqA*, *rep*, and *seqA rep* overnight cultures were diluted (100-fold for AB1157 and *rep* and 50-fold for *seqA* and *seqA rep*) and were shaken at 28° until A_{600} = 0.3. HU was then added to 10 mM, and the cultures were grown for an additional 4 hr at 28°. Samples were taken at time 0 (before HU addition) and after 4 hr, and the *ori/ter* ratio in the phenol–chloroform-purified chromosomal DNA from these cultures was measured using Southern hybridization, as before (Kouzminova and Kuzminov 2006; Rotman *et al.* 2014). Overnight (ori/ter = 1) and exponentially growing (ori/ter = 2) AB1157 cultures offered controls.

Chronic HU treatment

AB1157 overnight culture was diluted 1000-fold and shaken at 28° in the presence of 1, 3, 5 and 10 mM HU overnight. In the morning they were again diluted 100-fold and shaken for ~4 hr at 28° in the presence of 1, 3, and 5 mM HU. The 10-mM culture was very slow growing, and even the overnight culture had an OD of ~0.3 and therefore was allowed to grow for another 4 hr without dilution. The ori/ter ratio of these cultures was then measured using Southern hybridization.

Preparation of chromosomal DNA in agarose plugs (for subsequent PFGE or hybridization)

Strains were grown and processed under the conditions of a specific experiment. Samples in a volume of 0.2–4.0 ml were withdrawn at appropriate times, and cells were harvested by 1 min of centrifugation. The cell pellet was suspended in 120 μl of TE buffer (10 mm Tris–HCl and 1 mm EDTA, pH 8.0), mixed with 10 μl of 5 mg/ml proteinase K (Roche Applied Science) and 130 μl of molten (and cooled down to 70°) agarose in 0.2× lysis buffer (1.2% agarose in 1% lauroylsarcosine, 50 mm Tris–HCl, and 25 mm EDTA, pH 8.0) and quickly transferred to plug molds (Bio-Rad) in duplicate and allowed to set at room temperature for 2 min. Once solidified, the plugs were submerged in 1 ml of the lysis buffer (1% lauroylsarcosine, 50 mm Tris–HCl, and 25 mm EDTA, pH 8.0) and incubated overnight at 60°. After completion of digestion, the lysis buffer was replaced with TE buffer, and plugs were used immediately or stored at 4°.

Chromosomal fragmentation analysis

Labeling of the chromosomes was done by growing strains in the presence of 1–2 μCi/ml ^{32}P-orthophosphoric acid (MP Biomedicals or Perkin Elmer) at temperatures described in individual experiments. Once the cultures reached A_{600} = 0.2, they were split, and IPTG was added to 1 mM in one half. Both induced and un-induced cultures were further incubated, and samples for plugs were withdrawn at different times. Agarose plugs were prepared as described above and subjected to PFGE in a Bio-Rad CHEF-DR II system as described (Khan and Kuzminov 2012, 2013). Following completion of electrophoresis, the gel was dried under vacuum and subjected to autoradiography and quantification as described before (Khan and Kuzminov 2012, 2013).

Plug hybridization for ori and ter signals

Plug hybridization followed the published protocol (Kouzminova and Kuzminov 2012). The plugs with unlabeled chromosomal DNA were washed in glass tubes with two changes of 1 ml TE (30 min each) on a rotary shaker with gentle agitation. Following this, the plugs were treated sequentially with 1 ml each of 0.25 M HCl, 0.5 M NaOH, and 1 M Tris–HCl, pH 8.0, with each treatment lasting for 30 min. After the final wash, DNA from plugs was vacuum-transferred in two identical sets onto nylon membrane (Hybond H+, GE Biosciences) and UV-crosslinked to the membrane (UV Crosslinker FB-UVXL-1000, Fisher). After UV treatment, the membrane was cut into two halves to separate the sets of transferred DNA, and one-half was probed with a ^{32}P-labeled *oriC* probe, while the other half with the ^{32}P-labeled *dif* probe (Kouzminova and Kuzminov 2012). Hybridization was performed overnight at 63° in a 0.5 M sodium phosphate and 5% SDS hybridization buffer. In the morning the membranes

were washed thrice with 0.1× hybridization buffer and rinsed with deionized water just before covering them with Saran wrap and exposing them to a PhosphorImager screen. The resulting signals were measured with a PhosphorImager (Fuji Film FLA-3000) and normalized to those of AB1157 overnight cultures.

Marker frequency analysis

Chromosomal DNA for marker frequency analysis with deep sequencing was generated by phenol–chloroform extraction (Kouzminova and Kuzminov 2006) because we found that using commercial DNA purification kits leads to underrepresentation of specific genomic regions. Deep sequencing was done on the Illumina HiSeq2500 platform at the University of Illinois at Urbana-Champaign W. M. Keck Center for Comparative and Functional Genomics.

Sequence data were analyzed for quality using Fastqc (v0.11.2, http://www.bioinformatics.babraham.ac.uk/projects/fastqc). Reads were trimmed by Trimmomatic (v0.32) (Bolger *et al.* 2014) using TRAILING:30 MINLEN:91 parameters and analyzed a second time for quality with Fastqc. Trimmed reads were aligned to the *E. coli* K-12 MG1655 reference genome (National Center for Biotechnology Information taxid: 511145, accession: NC_000913.3) using bwa (v0.7.10) (Li and Durbin 2009) and aligned reads were converted from SAM to BAM format by samtools (version 0.1.19) (Li *et al.* 2009). Aligned reads were converted to absolute genomic coordinates with Novocraft's novosort (v3.02.08, http://www.novocraft.com). Per-base read depth was determined using genomecov from the bedtools software suite (v2.17.0) (Quinlan and Hall 2010), and resulting per-base "counts" were binned by calculation of mean read depth over contiguous 100-base intervals. The final step generated output in comma-separated-value format for import into Microsoft Excel. Binning the data set over 100-base intervals, and the accompanying 100-fold reduction in the size of the data set, was necessary for efficient manipulation of the output in Excel. Final output was a data set containing 46,417 entries with each entry consisting of per-bin genomic coordinates and mean read depth.

The filtering file that contains all annotated repeated regions, REP elements, *rrn* genes, and cryptic prophages was created. Filtering of these elements was necessary because the bwa program maps reads randomly and so produces anomalous read counts in bins overlapping multi-copy sequences. Collectively, a total of 3144 bins were removed from raw data counts in each strain as a result of repeat filtering.

The following additional deletions of the AB1157 strain were applied: Δ*gpt-proA*, Δ*lacA-lacY*, Δ*uxaB-yneF*, Δ*gadA-gadB* (coordinates: 255,900–262,800, 361,700–362,100, 1,610,300–1,611,000, 2,233,100–2,239,200) and the region *gadB* (1,570,700–1,571,700), which give abnormal high reads in all strains. The Δ*tnaA-tnaB* deletion with coordinates 3,888,800–3,890,600 was removed from all strains, except the SRK strains. Bins containing Δ*rep* (coordinates 3,930,900–3,940,500) were removed from the Δ*rep* strain. Deletion in *seqA* with coordinates 713,000–713,500 was not removed.

Regions removed (due to artificially high scores) from SRK strains were the following: 366300–367500 *lacI* (the integrated construct signal); 729,800–730,500 *rhsC*; 1,532,200–1,532,800 *ydcC*; and 732,000–732,200 putative transposon.

For plotting data, the signals were normalized to the *dif* area. Each raw data count was divided by the average value calculated for the 100-kbp region around *dif* (coordinates 15,288,800–1,652,800 with the corresponding cell number 13784 and 14784). These coordinates varied slightly for some mutants due to the deletions that they carry. Using Microsoft Excel, the moving average was produced using a window size of 100 (10 kbp).

Statement on data and reagent availability

Strains, plasmids, and sequencing data described in this article are available upon request.

Results

Formalism of static vs. dynamic CRC regulation

Formally speaking, regulation of chromosomal replication complexity could have either a static or a dynamic nature. A static regulation would be a dedicated system imposing a fixed limit that the chromosome is not allowed to cross. An obvious candidate for such a system in *E. coli* would be the eclipse system that determines the minimal distance between codirectional replication forks. The mechanistic enforcement of the limit would obviate the need for systems to sustain viability at higher levels of replication complexity or for recovery from an accidental crossing of the limit. The features of CRC that would be consistent with a static nature of CRC regulation include the following (Figure S1, left): (1) various mutants or conditions maximizing CRC to the same highest level; (2) existence of an optimum in conditions or mutation defects for the highest CRC, so that pushing cells past this optimum would inhibit cell growth and would actually decrease their CRC, both acting to preserve viability. These two features—similar maximal levels of CRC in different mutants/conditions and the peak-optimum nature of these maximal levels—define the static nature of CRC regulation in that both imply the presence of a dedicated system to impose the CRC limit. Put another way, when a system reacts to condition gradients by modulating its gross output around a local optimum, and these optima are similar under variety of conditions, this is indicative of a dedicated mechanism capable of recognizing these disparate challenges and, by integration of multiple inputs, of defining the optimal output of the critical parameter (CRC in this case).

In contrast, a dynamic CRC regulation would be a flexible one, in that there would be mutants or conditions with significantly increased, yet still varied, replication complexity, balanced by lower rates of growth. Because of this expected

inhibition, there would also be dedicated mechanisms to sustain the higher levels of replication complexity and to recover from crossing into the growth-inhibitory levels. The features of CRC that would be consistent with dynamic regulation include the following (Figure S1, right): (1) significant variations in CRC levels depending on mutants or conditions and (2) correspondence of the highest CRC to the slowest growth rate. In general, if a condition gradient induces a response gradient without a specific limit, this defines a system with dynamic response. Such dynamic response is based on the assumptions that the support mechanisms will help to survive the challenge and that the magnitude of the critical output will be a function of both the magnitude of the challenge and of the efficiency of specific mechanisms functioning to counteract the challenge.

Static features of the natural CRC limit

Even though the known CRC values in mutants or conditions (see the Introduction) do not distinguish between static *vs.* dynamic nature of the CRC limit in bacterial chromosomes, theoretical considerations suggest a static limit at two replication rounds (CRC = 4) (Zaritsky *et al.* 2006, 2007), while various mutants and conditions with CRC∼6 (Lane and Denhardt 1975; Martín and Guzmán 2011; Rotman *et al.* 2014) clearly violate this limit, suggesting its possible dynamic regulation. To gain insights into the nature of the CRC limit regulation in *E. coli*, we started with both mutants and conditions known to maximize replication complexity and then attempted to further elevate CRC.

We have verified the literature reports of the ori/ter ratio of 6–7 in the *rep* and *seqA* mutants (Figure 1, C and E). From our previous unpublished work we knew that the *seqA rep* double mutant is severely inhibited (Figure 1D); we suspected that the inhibition reflected a dramatically elevated CRC. However, the ori/ter ratio in this mutant turned out to be only ∼5.5 (Figure 1C), and although the difference from the *seqA* single mutants was barely significant, the same or decreased CRC in the double mutant was consistent with the existence of the chromosomal optimum for achieving the highest stable replication complexity in the *E. coli* chromosome (compare with Figure S1, the "2-left" scenario), pushing past which incurs penalties.

The static nature of the replication complexity limit in *E. coli* was further corroborated by the ori/ter ratio in wild-type cells grown for 4 hr (six regular doublings at 28°) in the presence of 10 mM HU. The DNA synthesis rate rapidly decreases upon 10 mM HU addition, but then starts recovering after 30 min of treatment (Figure S2). At this concentration of the replication inhibitor, division time becomes very long, even though replication forks can still slowly progress (Kuong and Kuzminov 2009, 2012), while no cell death is observed during this period of treatment (Sinha and Snustad 1972). We found that HU-treated wild-type cells reach the ori/ter ratio of 7–8 (Figure 1, C and E). Interestingly, the highest value reported for still growing cells in the literature is CRC∼8, observed during thymine starvation, when only one of 1000 cells remains viable (Martín and Guzmán 2011). Since these values are not much higher than the CRC values in *seqA* and *rep* mutants, yet are induced by metabolic conditions, rather than by DNA enzyme defects, these observations support the idea that the limit of replication complexity in the *E. coli* chromosome is mostly static in nature (a hard, mechanistic limit).

Comparison of the replication profiles of the *rep* and *seqA* mutants with wild-type cells, as well as wild-type cells growing in the presence of 10 mM HU for 4 hr, clearly shows the steady-state nature of chromosomal replication, with more numerous replication forks still evenly spaced along the chromosome (Figure 1E). We concluded that, while the rapidly growing wild-type cells have a single replication round per chromosome (Figure 1E, the blue profile), cells with inhibited replication forks maintain up to three replication rounds in their chromosome (Figure 1, E and F). Since three replication rounds per chromosome is the highest replication complexity in growing cells reported in the literature (Lane and Denhardt 1975; Martín and Guzmán 2011; Rotman *et al.* 2014), both our and the literature data suggest "CRC∼8" in *E. coli* as a natural limit showing static features.

Predictions of static vs. dynamic CRC regulation models

Before experimental challenge of the apparent static nature of CRC limit, we formulated expectations from the two modes of CRC regulation. There are at least three experimental predictions about the behavior of the static CRC limit under changing experimental conditions (the numbering continues from the formal analysis above) (Figure S1, left): (3) much higher CRC levels could be observed in mutants inactivating the system responsible for maintaining the limit; (4) cellular viability at the CRC limit would be independent of known support systems, but upon violation of the limit, viability would suffer; (5) the nature of the chromosomal replication profile should be steady-state (constant slope throughout the profile) even during transitions from one CRC to another because CRC limits (at any level) are enforced by an eclipse-like system that ensures the constant distance between replication forks.

There are also three contrasting predictions about the behavior of dynamic CRC regulation under changing experimental conditions (Figure S1, right): (3) the viability at the highest CRC levels would be dependent on support systems (such as DNA repair); (4) no particular mutants would dramatically elevate CRC beyond some higher values, but some growth conditions could, and this would not be lethal as long as the support systems are not overwhelmed; (5) the nature of the chromosomal replication profile would be non-steady-state (different slopes in different chromosomal regions), especially during the transitions from one CRC to another, as no specific system watches for constant distance between replication forks. Below our experiments with mutants, conditions and artificial constructs are matched with the contrasting expectations of the static *vs.* dynamic models of CRC regulation in *E. coli*.

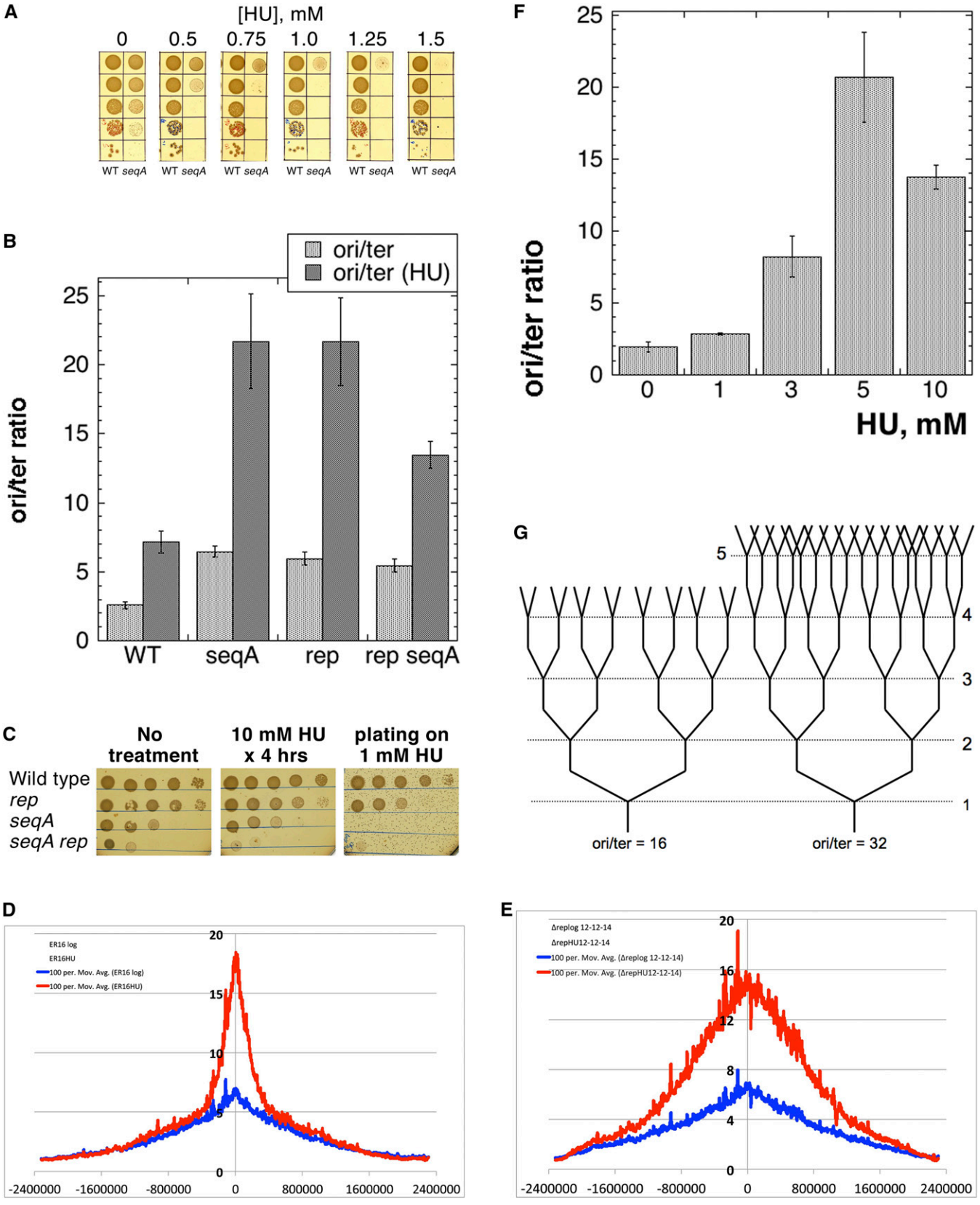

Figure 2 Breaking through the natural limit of chromosomal replication complexity reveals the "functional" CRC limit. (A) Inhibition of *seqA* mutant cells with concentrations of HU subinhibitory for wild-type cells. (B) Replication complexity in *seqA*, *rep*, and *seqA rep* mutant cells treated with 10 mM HU for 4 hr. Data for wild-type (HU) and for untreated mutants are from Figure 1B. (C) Survival of the cells from cultures either treated with 10 mM HU for 4 hr or spotted on LB + 1 mM HU. (D) Chromosomal marker-frequency profiles of the untreated *seqA* mutant (blue trend line) *vs.* the *seqA* mutant

Breaking through the natural CRC limit reveals the functional CRC limit

The slow-growing *seqA* mutants are sensitive to HU (Sutera and Lovett 2006) and are synergistically inhibited by 1 mM HU, the concentration at which wild-type cell growth is unaffected (Figure 2A). To test the static nature of CRC∼8 limit, we inhibited DNA synthesis in *seqA* and *rep* single mutants, as well as in *seqA rep* double mutants, with 10 mM HU for 4 hr. We expected that this treatment, which allows only minimal DNA replication (Figure S2), would not increase CRC past the suspected maximum of 8, while grossly inhibiting and even killing the two mutants. Surprisingly, both the *seqA* and *rep* mutants acutely treated with HU increased ori/ter to ∼22 (Figure 2B). The *rep seqA* double mutant showed a more modest CRC increase (ori/ter ∼13) (Figure 2B). Although no culture growth was observed under these conditions, survival of the cells (titer of the cultures) was not affected by this acute HU treatment (Figure 2C), indicating that the cells can completely recover from this serious breach of CRC∼8 limit. Moreover, chromosomal marker frequency profiles of *seqA* and *rep* mutant cells after growth for 4 hr in the presence of 10 mM HU featured at least two distinct slopes and therefore were obviously non-steady-state (Figure 2, D and E), suggesting a breakdown of the system that maintains constant distance between codirectional replication forks. Thus, inconsistencies with the static nature of the CRC∼8 limit included: (1) breaching of the limit by conditions (even though in specific mutants); (2) no accompanying loss of viability; (3) the non-steady-state nature of the replication profiles. This transient condition-dependent nonlethal increase of the CRC limit to between four and five replication rounds per chromosome (Figure 2G) argues for dynamic regulation of the CRC limit in *E. coli*.

The increased CRC∼22 was due to the combination of HU treatment with the *seqA* or *rep* defects (conditions + mutations), since CRC was only 7 in the wild-type cells similarly treated with HU for 4 hr (Figure 2B). To test if the wild-type cells would still saturate CRC at ∼8 during continuous HU treatment (conditions only), we grew wild-type cells for up to 20 generations in the presence of varied concentrations of HU, up to 10 mM (Figure 2F). Longer growth in liquid cultures was impractical because of eventual overgrowth by HU-resistant mutants. We found that the previous CRC∼8 limit was stably maintained at 3 mM HU. Surprisingly, ori/ter ratios reached >20 in cultures grown in the presence of 5 mM HU, consistent with the existence of the higher CRC limit of 22, detected in the *seqA* and *rep* mutants. At the same time, the cells growing extremely slowly in the presence of 10 mM HU showed a decreased replication complexity of ∼13 (Figure 2F). We conclude that: (1) severe inhibition of replication forks (the *seqA rep* double mutant or wild-type cells grown in the presence of 10 mM HU) decreases replication complexity below the maximal one (in other words, maximal replication complexity requires "optimal" replication inhibition), as if severe inhibition of replication elongation also affects initation efficiency; (2) the higher CRC∼22 limit is independent of the SeqA or Rep status of the cells and functions as a higher limit of static nature. Overall, we conclude that the *E. coli* chromosome not only has the natural CRC∼8 limit, but can be pushed to the "functional" CRC∼22 limit corresponding to between four and five replication rounds per chromosome (Figure 2G). These complex and intriguing results suggest that both static and dynamic aspects regulate high replication complexity limits in *E. coli* cells.

A system to maximize CRC

The fact that high chromosomal replication complexity is associated with inhibited cell growth suggests a decreased functionality of the chromosome and implies formation of chromosomal lesions. Indeed, both the HU treatment, on the one hand, and the *seqA* and *rep* defects, on the other hand, induce formation of double-strand DNA breaks (Michel *et al.* 1997; Mohana-Borges *et al.* 2000; Rotman *et al.* 2014), perhaps the most serious of all chromosome lesions (Resnick 1978; Iliakis 1991). At the same time, both the natural CRC∼8 and the functional CRC∼22 limits are well-tolerated, suggesting robust chromosomal repair mechanisms. Therefore, we have expanded the last initial objective of our study, which was to determine the nature of growth inhibition during elevated CRC. Our three new objectives were to investigate the following: (1) the nature of chromosomal lesions associated with high CRC; (2) the mechanisms (avoidance or repair) allowing cells to tolerate high CRC; (3) the nature of irreparable chromosomal damage caused by the maximal CRC. The third objective reflected our expectation that breaking through the functional CRC∼22 limit, if proved possible, would result in cell lethality due to particular chromosomal problems, which we could characterize.

Because we suspected that high CRC induces chromosome fragmentation, making cells dependent on double-strand break repair catalyzed in *E. coli* by the RecBCD pathway (Kuzminov 1999, 2011), we could not genetically explore high CRC tolerance using the *seqA* and *rep* mutants, as both depend on the RecBCD pathway for viability (Uzest *et al.*

treated with 10 mM HU for 4 hr (red trend line). (E) Chromosomal marker-frequency profiles of the untreated *rep* mutant (blue trend line) *vs.* the *rep* mutant treated with 10 mM HU for 4 hr (red trend line). (F) CRC in wild-type cells growing at steady state in the presence of the indicated concentrations of HU. An overnight culture of AB1157 was diluted 1000-fold and split into several subcultures grown in the presence of the indicated HU concentrations for 24 hr. Subcultures that reached saturation were again diluted 100-fold into the same media and grown for ∼4 hr. The 10 mM culture grew extremely slowly and was not diluted the second time, but just grown for another 4 hr. Kinetics of OD increase of the cultures were monitored, as well as the shape of the cells under the microscope, to guard against a sweep by HU-resistant mutants. (G) Schematic chromosomal replication complexity at ori/ter = 16 and 32.

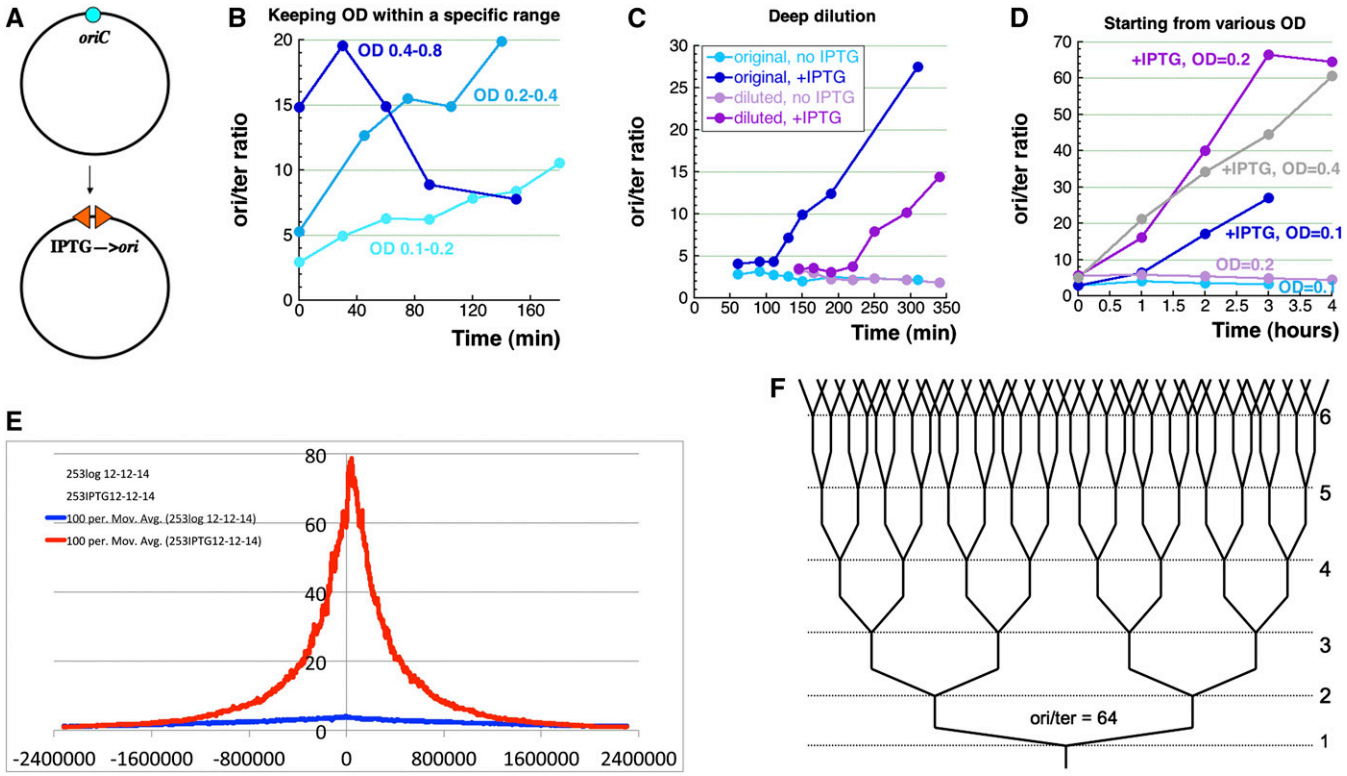

Figure 3 Finding optimal induction conditions for maximal ori/ter ratio with inducible chromosomal origin. All cultures in this figure and in Figure 4 and Figure 5 were grown at 37° to fully inactivate the *recBC*(Ts) allele, if present. At 37°, the wild-type doubling time is ~25 min, elevating the basal ori/ter ratio to almost 4. (A) A scheme of the chromosome driven by IOC, which is the double back-to-back IPTG-driven ColE1 origin, inserted ~5 kbp "to the right" of *oriC*, which is still there. (B) Optimizing the induction 1: keeping OD of the induced culture within specific ranges. In B–D, the strains were either SRK252 or SRK253, as they behaved essentially the same. (C) Optimizing the induction 2: deep dilution of the culture. An overnight culture was diluted 100-fold ("original culture"), grown for 2 hr, then a portion of it was further diluted 400-fold (at the time point of 120 min), and both the just-diluted and the original cultures were induced with IPTG at that time. (D) Optimizing the induction 3: starting induction from cultures with various (indicated) ODs. (E) Chromosomal marker-frequency profiles of the wild-type (blue) and IOC (red) strains after 4 hr of IPTG induction from OD = 0.2. (F) Schematic chromosome replication complexity at ori/ter = 64.

1995; Kouzminova *et al.* 2004). Therefore, to specifically address our new objectives, we built an experimental system with conditional (inducible) high CRC by inserting an inducible bidirectional replication origin near *oriC* (Figure 3A). For this, we reconstructed a plasmid with an IPTG-driven unidirectional replication origin (Gil and Bouché 1991) to carry two back-to-back IPTG-inducible origins, separated by a 2-kbp fragment of chromosomal DNA from a position 5 kb away from *oriC* and forced integration of the resulting plasmid into the chromosome by keeping selection for the plasmid-borne *bla* gene in the absence of IPTG (Figure S3). Finally, to stabilize this IOC in the chromosome and to mark it further, we replaced one of the two chromosomal DNA repeats with the *kan* gene (Figure S3).

Since our *recBC*(Ts) allele is fully a *recBC* mutant at 37° (Kushner 1974), we experimented with IPTG-inducible origin (in wild-type cells) at 37°. We tried several conditions for inducing maximal replication complexity in the resulting IOC strain with IPTG, but at first our repeated attempts failed to approach even the CRC = 30 level by the time the induced cultures saturated, supporting the reality of the functional CRC~22 limit. If we kept the cultures after IPTG addition in a particular OD range by regular dilutions, the ori/ter ratio in the IOC strain increased slowly at OD = 0.1/0.2, increased faster at OD = 0.2/0.4 (promising, but still not practical at this point), but actually started decreasing at higher ODs (Figure 3B). If we diluted the IOC culture deep before IPTG addition, the ori/ter ratio increase was delayed until the diluted cultures reached OD ~0.2, but then was delayed again upon re-dilution (Figure 3C), again pointing to OD = 0.2 as the "magic spot" for IPTG-induced overreplication.

The surprisingly narrow optimum of OD = 0.2 for maximizing the inducible origin firing was eventually confirmed by adding IPTG at various ODs to aliquots of the IOC culture that was diluted once from an overnight culture (Figure 3D). The ori/ter ratio reached 60–80 under these growth conditions (Figure 3, D and E), with an average maximal CRC~64 translating into six replication rounds (Figure 3F). The replication profile of such a hyper-initiated chromosome looked distinctly non-steady state, indicating that, even after 4 hr of induction, the replication forks were reaching only to the middle of the replichores (Figure 3E). The CRC~64 was a maximum after 4 hr of induction because the IOC cultures

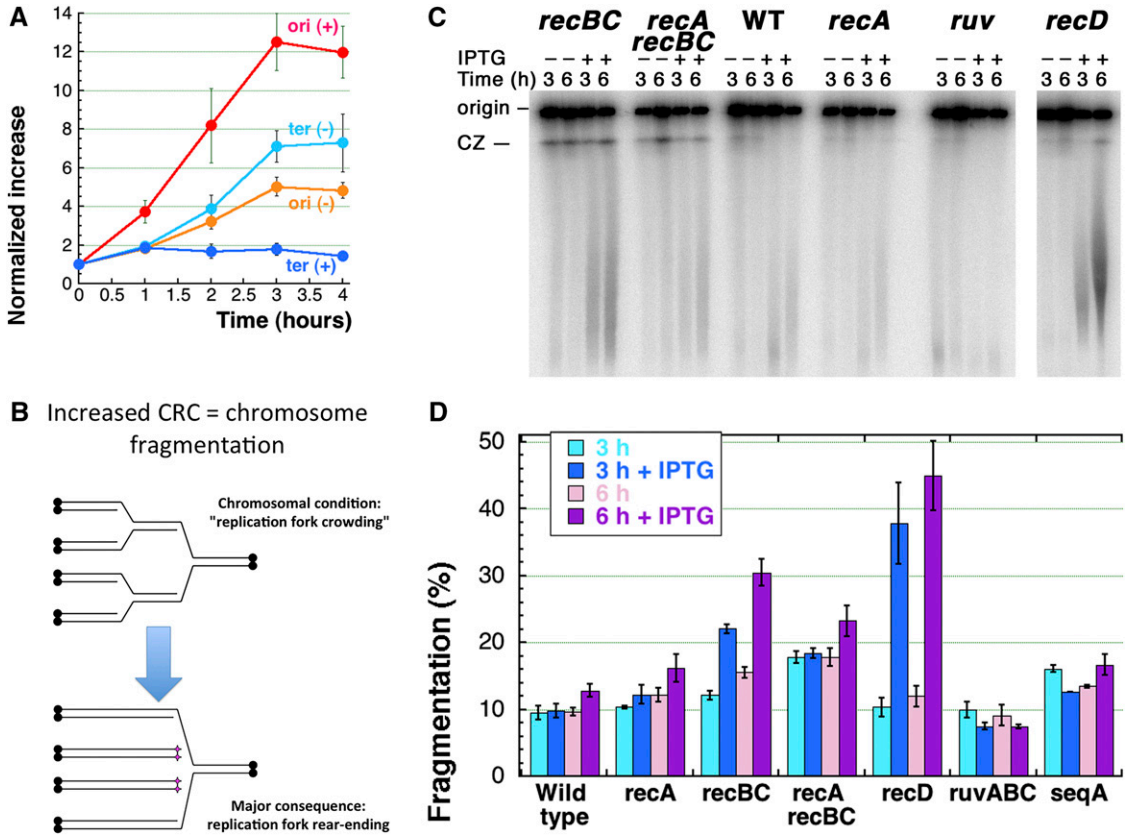

Figure 4 Chromosome fragmentation due to the induced overinitiation. (A) Kinetics of origin and terminus accumulation in the absence of induction (–) *vs.* after IPTG induction (+). The apparently low numbers for origin increase in the IPTG-induced cultures (12× over the initial level) actually match the high ori/ter ratios from Figure 3D because the initial ori/ter ratio (6 in this experiment) should be used as a multiplier. (B) A scheme of how replication fork crowding can lead to double-strand DNA breaks via replication fork rear-ending into each other. (C) A representative pulsed-field gel to detect chromosomal fragmentation in various *rec* mutants carrying the inducible origin. CZ, compression zone. The resolution of these gels is such that the bottom corresponds to ~50 kbp, while the compression zone accumulates species that are ≥2 mbp (Kouzminova *et al.* 2004). (D) Quantification of chromosomal fragmentation at 3 hr (3 h) and 6 hr (6 h) of IPTG induction in various mutants carrying inducible origin. The corresponding uninduced controls (light color bars) serve as a background. Data are means of three to eight independent determinations ± SEM.

would reach saturation, while further incubation (overnight) would lead to lower ori/ter ratios (most likely due to terminus replication with no further initiations). IPTG induction in wild-type cells at 28° showed a slightly slower kinetics of CRC increase (Figure S4), so all our subsequent experiments were done at 37°. Having an experimental system in which such a runaway (uncontrolled) overinitiation pushed the chromosomal replication complexity over the functional CRC~22 limit to the new CRC~64 limit allowed us to address our new objectives centered around characterization of chromosomal lesions.

Runaway CRC fragments the chromosome

While the ori/ter ratio indicates chromosomal replication complexity, separate kinetics of normalized accumulation of the terminus DNA relative to the origin DNA reflect the status of replication forks. In the typical growing cultures reaching saturation, normalized terminus accumulation eventually overshoots the normalized origin accumulation (Figure 4A, (−) curves) because they start at ori/ter = 2 in the growing cells, but should reach ori/ter = 1 at saturation. In contrast, upon IPTG induction in the IOC strain, while origin-specific DNA accumulates according to the kinetics of ori/ter ratio increase, the cessation of terminus-specific DNA accumulation in response to IPTG induction confirms replication forks failing to reach the terminus (Figure 4A, (+) curves). Thus, runaway CRC severely inhibits replication forks.

Inability of replication forks to reach the terminus means that they are inactivated. Since the obvious type of chromosomal condition due to high CRC is "replication fork crowding" (Table S2), the suspected major consequence would be replication forks rear-ending into each other to generate double-strand DNA breaks (Bidnenko *et al.* 2002; Rotman *et al.* 2014) (Figure 4B). Thus, the inability of replication forks to reach the terminus under conditions of runaway CRC may be similar to the situation in the *dut recBC* mutants, where replication forks succumb to chromosome fragmentation detectable in pulsed-field gels (Kouzminova and Kuzminov 2006). However, we detected very little chromosome fragmentation in the IOC strain upon IPTG induction ("WT" and "Wild type" in Figure 4, C and D), perhaps because of its low level in combination with efficient repair.

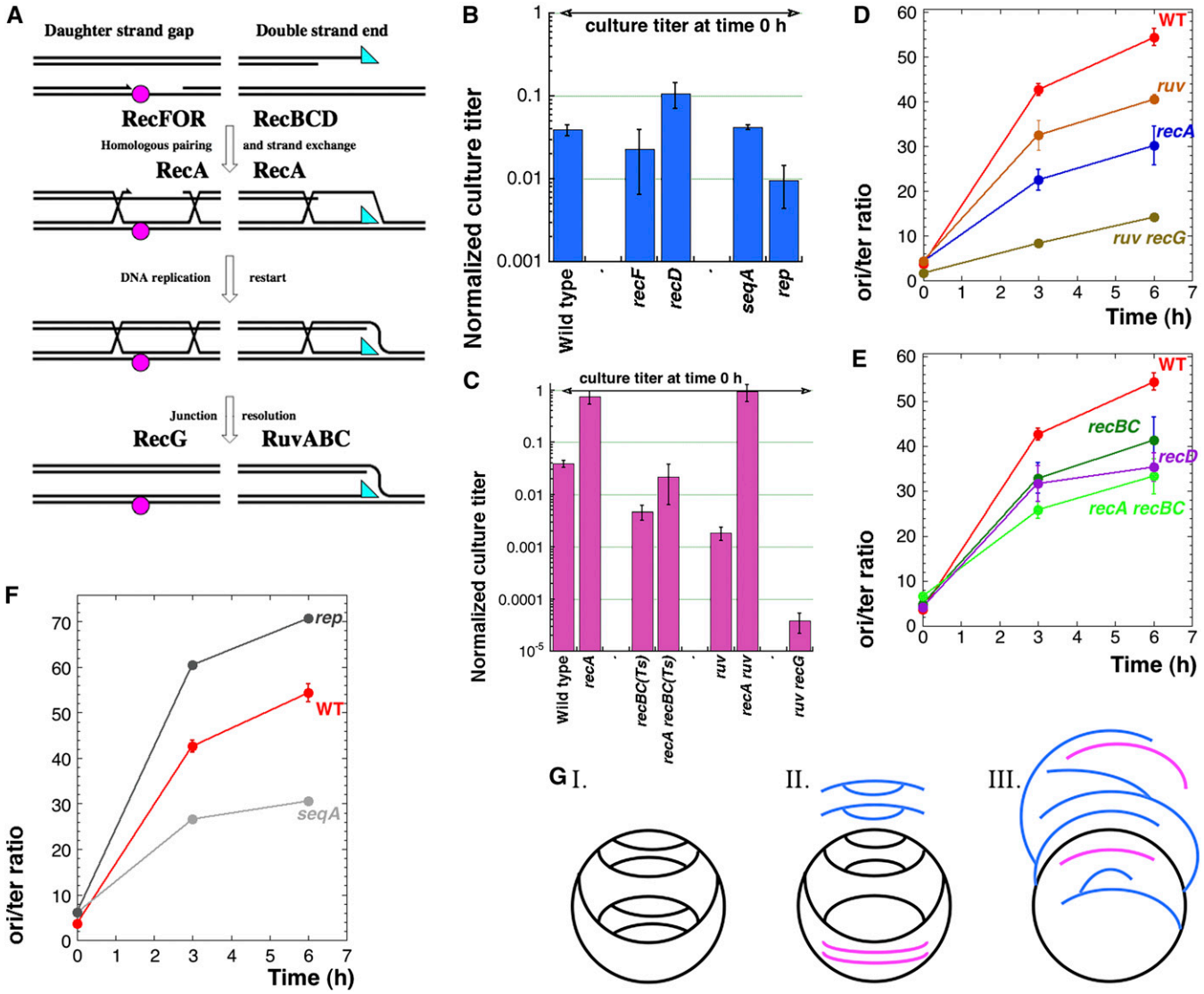

Figure 5 Genetics of survival of the induced overinitiation *vs.* the kinetics of CRC accumulation. (A) A scheme of the two major pathways of recombinational repair in *E. coli*. Magenta circle, a noncoding DNA lesion; cyan triangle, the invading 3′-single-strand end. (B) Survival of 6 hr IPTG induction by wild-type and various mutant IOC cultures with wild-type-like effects. (C) Survival of 6 hr IPTG induction by wild-type and various double-strand break repair-mutant IOC cultures. (D) Kinetics of the ori/ter ratios during IPTG induction of IOC in wild-type cells, as well as in *recA*, *ruv*, and *ruv recG* mutants. (E) Kinetics of the ori/ter ratios during IPTG induction of IOC in recBC(Ts), *recA recBC*(Ts), and *recD* mutants. (F) Kinetics of the ori/ter ratios during IPTG induction of IOC in *rep* and *seqA* mutants. (G) A scheme of possible chromosome problems due to runaway CRC. DNA duplexes are presented by single lines. Black lines, the circular domains of the chromosome; blue lines, the (partially) linear domains that would not enter pulsed-field gels; the pink lines, subchromosomal fragments that would enter pulsed-field gels. Scenario I: The overreplicating chromosome without problems and lethality. Scenario II: Some replication forks rear-ended the previous forks in a paired fashion, while (in the top half) new initiations also happened, masking some fragmentation. Similar to scenario I, this scenario also predicts no lethality, even without any further action form the cell. Scenario III: Unpaired replication fork disintegration generates multi-tailed chromosome (expected to be lethal without repair or linear DNA degradation).

To detect low-level chromosomal fragmentation in *E. coli*, both linear DNA degradation and its recombinational repair have to be blocked with a *recBC* mutation (Michel *et al.* 1997; Kouzminova *et al.* 2004; Khan and Kuzminov 2012) (Figure 5A). Indeed, we found modest levels of chromosomal fragmentation [reaching ~15% over the background after 5–6 hr of IPTG induction (Figure S5)] to develop in the IOC *recBC* mutant, compared to <5% in the wild-type cells, *recA*, *ruvABC*, and *seqA* mutants (Figure 4, C and D). The modest levels of this fragmentation were far from the immediately lethal catastrophic fragmentation levels observed with some DNA-damaging treatments (Khan and Kuzminov 2013; Mahaseth and Kuzminov 2015) and predicted an equally modest effect on the actual survival. At the same time, the IPTG-induced IOC *recD* mutant (reduced for linear DNA degradation, but enhanced for repair of double-strand breaks) showed a 2× higher fragmentation (>30%) (Figure 4, C and D), suggesting that, in the case of runaway CRC, linear DNA

degradation is more useful than double-strand break repair for keeping chromosomal fragmentation under control.

Recombinational misrepair at high CRC and the help from linear DNA degradation

The observed chromosomal fragmentation in the *recBCD* IOC mutants, and the absence of it in the RecBCD+ IOC strain, suggested that the viability of cells with runaway CRC should depend on recombinational repair of double-strand breaks. There are two pathways of recombinational repair in *E. coli*: the RecFOR-promoted repair of blocked single-strand gaps and the RecBCD-promoted repair of double-strand ends (Figure 5A). In addition to these pathway-specific genetic requirements, both pathways depend on the RecA-catalyzed homology-guided strand exchange and on the RuvABC/RecG-catalyzed removal of DNA junctions (Kuzminov 1999, 2011). Indeed, the *recBC* mutant was losing viability upon IPTG induction (0.5% survival after 6 hr of IPTG induction) (Figure 5C), suggesting that at least some of the observed double-strand breaks do inactivate the chromosome. Surprisingly, the DSB repair-proficient wild-type or *recF*-mutant IOC cultures also lost viability to a significant degree (2–4% survival after 6 hr induction) (Figure 5, B and C), suggesting that normal repair of the induced double-strand breaks still fails to restore chromosome functionality. The "high-CRC" *seqA* and *rep* mutants also showed a similar level of survival, 5 and 1%, correspondingly (Figure 5B).

Double-strand break formation and repair happened as a result of runaway CRC because: (1) survival of repair-enhanced but linear DNA degradation-defective *recD* mutants was better than that of wild-type cells (Figure 5B); (2) the *ruvABC* and *ruvABC recG* mutants, correspondingly defective and deficient in the late stages of double-strand break repair (Figure 5A), were killed much deeper than *recBC* mutants that block repair at early stages (Figure 5C), indicating robust formation of DNA junctions during this repair. At the same time, the *recA* mutants, deficient in the central stage of recombinational repair (Figure 5A), showed almost no death after 6 hr of induction (Figure 5C), suggesting that to ignore double-strand breaks in this situation is better than to repair them. Interestingly, compared to the vastly different survival levels of *recA* or *recBC* single mutants, the *recA recBC* double mutant shows survival closer to the one of the *recBC* mutant (Figure 5C), suggesting that it is the RecBCD-dependent degradation of linear DNA that allows the *recA* single mutant to survive induced overreplication. At the same time, the *recA* defect completely suppressed the poor survival of the *ruv* mutant (Figure 5C), confirming that, under the conditions of runaway CRC, recombinational repair becomes poisonous, and the cells are better off simply degrading linear DNA.

We tested a possibility that the differences in survival of runaway CRC either reflect or translate to the difference in maximal CRC induction. We found that the final CRC levels were indeed significantly lower in the *recA* mutant compared to wild-type cells (Figure 5D) and somewhat lower in the *recA recBC* mutant compared to the *recBC* mutant (Figure 5E), suggesting that recombinational repair poisons indirectly via repairing and restarting disintegrated replication forks (thus boosting the final induced CRC levels). The *recD* mutant also shows lower CRC levels (Figure 5E), but higher survival than the wild-type cells. The modest difference in survival between the *seqA* and the *rep* mutants (Figure 5B) could be also due to the significant difference in the final CRC after induction (Figure 5F). However, the same logic fails in the case of *recBC*, *ruv*, and *ruv recG* mutants, which all have the lowest survival levels (Figure 5C), but also decreased CRC levels (Figure 5, D and E).

Overall, we conclude that lower induced CRC levels do not necessarily save (especially evident in the case of the *ruv recG* mutant) and instead generally reflect the support of runaway CRC by functional recombinational repair of double-strand breaks. The corollary of the almost 100% survival of recombinational repair-deficient but linear DNA degradation-proficient (*recA*) mutants is that, during the runaway CRC, the double-strand breaks (1) form only in the replicated part of the chromosome; (2) do not affect the circular part of the chromosome; (3) generate ends that have to be either repaired or degraded for the cells to survive and, therefore, most of them must be still attached to the circular part of the chromosome (Figure 5G, III).

Discussion

We define CRC as the ratio of the copy number of the most replicated regions to that of unreplicated regions on the same chromosome. The origin of CRC definition can be traced to "chromosome complexity" of Itsko and Schaaper (2014) and "nucleoid complexity" of Zaritsky *et al.* (2007). Our experimental inquiry into the nature and scale of the CRC limit in *E. coli* produced an unexpectedly elaborate answer: (1) *E. coli* cells can be forced to reveal three CRC limits: ~8, ~22, and ~64; (2) each of these limits has static features in that it is reproducible with various strains/conditions and behaves like a local optimum; (3) the very fact that there are three limits instead of one indicates dynamic aspects in the regulation of elevated CRC; (4) dependence on recombinational repair of cells at the natural CRC~8 limit (and likely at the functional CRC~22 limit) and on linear DNA degradation of cells at the tolerance CRC~64 limit is also a dynamic feature of increased CRC management.

Multiple reports suggest that *E. coli* considers CRC~8 as the natural limit, approaching it readily in certain mutants/conditions (Lane and Denhardt 1975; Martín and Guzmán 2011; Rotman *et al.* 2014). Moreover, we have found that *E. coli* can still slowly grow at CRC~22, designating it as the functional CRC limit in this organism. When the cells develop the maximal ori/ter ratio of ~64, they stop multiplying, apparently because their replication forks experience problems reaching the terminus and pile up in the origin-centered 1/3 of the chromosome (Figure 3E). One of 20 wild-type cells survives CRC~64, making it the tolerance limit of replication complexity. At the same time, the *recA* mutant cells survive

runaway overinitiation in their chromosome without much problem (Figure 5C), possibly by keeping the actual chromosomal replication complexity closer to the functional CRC~22 limit (Figure 5D).

In general, survival at the tolerance CRC limit depends mostly on linear DNA degradation and partly on the double-strand break repair proficiency, suggesting formation of repairable double-strand breaks in the replicated part of the chromosome that still leaves the circular chromosome frame intact. When both double-strand break repair and linear DNA degradation are inactivated in cells with runaway overinitiation, subchromosomal DNA fragments are indeed detected by pulsed-field gels (Figure 4, C and D). Interestingly, the levels of chromosomal fragmentation induced by runaway overinitiation are moderate compared to some DNA-damaging treatments (Khan and Kuzminov 2013; Mahaseth and Kuzminov 2015), suggesting circular chromosomes with multiple linear tails as the main chromosome state (Figure 5G, III). Another factor likely diminishing the actual fragmentation levels is new initiation on subchromosomal fragments (Figure 5G, II), which will block their entrance into pulsed-field gels. Similar to *E. coli*, overreplication (called "rereplication" in eukaryotes) induces chromosomal fragmentation in mammalian cells, which is also mended by recombinational repair (Hook *et al.* 2007; Truong *et al.* 2014).

In fact, elevated chromosomal replication complexity is by no means a solely prokaryotic phenomenon. High local CRC, historically known as the "onion-skin DNA replication," is observed in eukaryotic cells at sites of chromosomal integration of papillomavirus and poliomavirus genomes (Syu and Fluck 1997; Kadaja *et al.* 2009), as well as at "puffs" of developmentally regulated local chromosome amplifications in insects (Spradling 1981; Liang *et al.* 1993). There is also a possibility that stable elevated replication complexity explains certain cases of copy number variation in cells of higher eukaryotes and the origin of certain chromosome rearrangement events (Hastings *et al.* 2009; Zhang *et al.* 2009). The role of increased CRC (re-replication) in carcinogenesis has been recently highlighted (Hook *et al.* 2007; Truong *et al.* 2014).

Runaway overinitiation disturbs both the CRC-limiting system and the chromosome cycle

Our results with slowly replicating mutants and conditions (Figure 1 and Figure 2) shed light on the nature of the CRC-limiting system. The initial idea was that the eclipse mechanisms would determine the minimal spacing between replication rounds, preventing this spacing from decreasing below a certain distance. If the eclipse system still works at higher CRC levels, the spacing between replication rounds should still be uniform, reflected in uniform slopes of the marker frequency gradients from the origin to the terminus. This is exactly what we observe at the natural CRC~8 limit (Figure 1D). But a different pattern develops at the functional CRC~22 limit: the HU-treated *seqA* mutants (Figure 2D) accumulate replication bubbles in the origin-centered 1/6 of the chromosome, corresponding to the origin macrodomain of the *E. coli* chromosome (Espéli and Boccard 2006), with apparently no consequence for long-term survival once the treatment is terminated. Similar replication bubble pile-up was noted before in the wild-type cells severely inhibited by 80 mM HU (Kuong and Kuzminov 2012). Such a "replication pile-up" suggests disappearance of the eclipse phenomenon in HU-treated cells, especially in the absence of SeqA, apparently due to the very slow movement of replication forks in the origin macrodomain. In other words, SeqA appears to assist replication fork movement through the origin macrodomain. At the same time, a similar-scale pileup appears to be partially resolved by 4 hr in the HU-inhibited *rep* mutants (Figure 2E), while wild-type cells show an essentially steady-state profile after the same HU treatment (Figure 1D), suggesting normal operation of the eclipse system and confirming SeqA as its major determinant.

During the runaway overinitiation (at the tolerance CRC~64 limit) we observed an exponential piling up of replication bubbles around the origin, with limited progress beyond the origin-centered one-third of the chromosome (Figure 3E). In place of the nonfunctional eclipse system (that regulates initiation frequency only at *oriC*), the replication complexity in this situation appears to be limited by availability of replication enzymes and proteins, and once the limiting component is exhausted, new replication rounds stop initiating, curbing further ori/ter ratio increase. Since the copy number of replication proteins/enzymes per cell is not known to be regulated by availability of their substrates (the replication fork structures), the limiting factors should be searched among the replication genes that are farthest on the chromosome from the (inducible) replication origin (whose copy number is therefore not elevated by overinitiation). Even if the replisome copy number is not regulated by the availability of its unoccupied replication fork structures, it may still be regulated by the overall DNA mass/concentration per cell. In addition, expression of some replisome genes is known to be upregulated by DNA damage (Kaasch *et al.* 1989; Kleinsteuber and Quiñones 1995; Courcelle *et al.* 2001). It could be also that the limiting factor is availability of the DNA precursors (dNTPs), whose pools may be anchored to the cell size, rather than to the number of replication forks.

The bacterial chromosome cycle (Kuzminov 2013, 2014) is distinct from the eukaryotic one in that segregation shortly follows replication, separated from it by a 5- to 10-min-long period of sister-chromatid cohesion (Viollier *et al.* 2004; Nielsen *et al.* 2007; Vallet-Gely and Boccard 2013). Stalling of replication forks or accumulation of single-strand interruptions behind the forks in bacteria, therefore, leads to catastrophic chromosomal consequences, reflected in such phenomena as thymineless death (Kuong and Kuzminov 2012), ligase-deficient death (Kouzminova and Kuzminov 2012), or sensitivity of *seqA* mutants to DNA damage (Sutera and Lovett 2006) and to rapid growth (Rotman *et al.* 2014). If chromosome segregation is still concurrent with replication in the cells with elevated CRC, the viability is expected to be

unaffected, as is indeed observed at the natural and functional CRC limits. In contrast, the decreased survival during runaway CRC suggests a partial breakdown of the replication–segregation tandem of the bacterial chromosome cycle and less efficient segregation under these conditions. The segregation problems will make faithful recombinational repair problematic, contributing to a peculiar high CRC-based phenomenon that we will discuss next.

Recombinational misrepair

Our observation that runaway overinitiation kills recombinational repair-proficient cells, but cannot kill repair-deficient yet linear DNA degradation-proficient *recA* mutant cells, indicates that recombinational repair becomes poisonous during maximized CRC. The dramatically decreased survival of runaway overinitiation by the mutants that cannot resolve DNA junctions indicates a massive recombinational repair effort and calls for an idea about a possible nature of recombinational misrepair. This idea needs to explain how an enzymatically and mechanistically sound reassembly of disintegrated replication forks may still produce a nonfunctional chromosome. One such idea envisions recombinational double-strand end repair attaching the broken end to a cousin duplex, instead of the sister one (Figure 6, C and D), the situation ending in formation of pince-nez chromosome (Figure 6E). Indeed, in a chromosome with CRC = 2 (Figure 6A), the only available duplex to reattach the double-strand end to after replication fork disintegration is the sister duplex, while in a chromosome with CRC = 4 (Figure 6B), this intact sister (theoretically) has to compete with two cousin duplexes of identical DNA sequence. Normally, sister-chromatid cohesion, although extremely short in bacteria (Kuzminov 2013, 2014), would still guide the repaired double-strand end toward the sister, while the concurrent segregation (Viollier *et al.* 2004; Nielsen *et al.* 2007; Vallet-Gely and Boccard 2013) will physically separate cousins, making them even less available. However, in conditions of CRC soaring beyond the control of the eclipse system, the now unregulated distance between replication forks may become too short, reducing sister-chromatid cohesion to a minimum. The situation is further exacerbated during runaway overinitiation by availability of multiple cousins and by their inefficient segregation.

Even though formation of pince-nez chromosomes had been already proposed (Russo *et al.* 1992; Smith 2012), and even reported in plasmids (Petes and Williamson 1994), possible mechanisms of their resolution are currently unknown. Thus, until such resolution mechanisms are found, tying up the replicating chromosome mass in pince-nez structures may be considered a lethal event and a general explanation for the toxicity of maximized CRC in recombinational repair-proficient cells. Conceptually, the pince-nez chromosome situation is similar to the "sigma-replication trap" (Kuzminov 1999; Miranda and Kuzminov 2003) in that a circular chromosome becomes trapped in unproductive replication if it develops an odd number of replication forks. We suspect that structures like pince-nez chromosomes are responsible for the phenomenon of inducible stable DNA replication in *E. coli*, observed after massive DNA damage in cells with blocked initiation of chromosomal replication from the origin (Kogoma 1997).

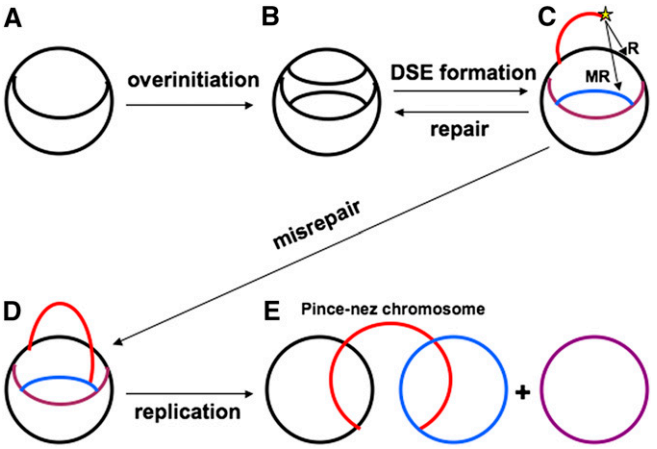

Figure 6 A model for recombinational misrepair: attachment of a double-strand end to a cousin duplex, rather than to the sister duplex. In some panels, chromosomal arms are color-coded to facilitate tracking. (A) A theta-replicating chromosome with CRC = 2. (B) Overinitiation increases CRC to 4. (C) Disintegration of one of the replication forks generates a double-strand end (DSE, marked with yellow star) that needs to be reattached by homology to restore the replication fork. Because of the increased CRC, there are three homologous duplexes: the sister one (black) and two cousins (blue and purple). R, reattachment to sister will be "repair" and will restore the structure in B. MR, attachment to one of the cousins will constitute "misrepair" and will lead to the structure in D. (D) A replicating chromosome with an inter-cousin arm. (E) Replication of this chromosome leads to four chromosomes: a free one (purple) and the "pince-nez" structure, linking circular black and blue chromosomes with a linear concatemeric red chromosome. How such a structure can be resolved is currently unknown.

In conclusion, when challenged, *E. coli* cells reveal at least three stable chromosomal replication complexity maxima in their chromosome: the natural CRC∼8 limit, the functional CRC∼22 limit, and the tolerance CRC∼64 limit. The behavior of individual CRC limits is consistent with their static nature, while the existence of three distinct CRC limits is consistent with their dynamic regulation. Since we suspect that the observed CRC limits beyond the natural one could be due to the segregation capacity of the cell or due to availability of replication proteins or DNA precursors, in the future it would be important to determine the following in cells with runaway CRC: (1) the cell volume relative to the nucleoid size; (2) the distribution of replication origins over the cell (or nucleoid) volume; (3) the DNA precursor pools; and (4) the copy number of the replisome components. On the other hand, it would be also interesting to determine the effects of the elevated replication complexity on various aspects of genome stability, including mutations and chromosomal rearrangements, as well as regulation of gene expression (a possible dosage compensation system in *E. coli*?). This modeling of runaway replication complexity in bacteria should also provide insights into locally amplified CRC of the eukaryotic onion-skin replication, as well as into CRC variation in cancer cells.

Acknowledgments

We thank Ella Rotman for providing Figure 2A; Massimo Lopes, Sue Lovett, Sergei Mirkin, Houra Merrikh, Chris Pearson, Tom Petes, Polina Scherbakova, Jeff Strathern and Jade Wang for their interest in this work and helpful suggestions; and Bénédicte Michel for many insightful comments that significantly clarified our presentation. This work was supported by grant no. GM 073115 from the National Institutes of Health. The funders had no role in study design, data collection and analysis, decision to publish, or preparation of the manuscript. The authors declare no conflict of interests.

Literature Cited

Ahmad, S. I., S. H. Kirk, and A. Eisenstark, 1998 Thymine metabolism and thymineless death in prokaryotes and eukaryotes. Annu. Rev. Microbiol. 52: 591–625.

Atkinson, J., M. K. Gupta, and P. McGlynn, 2011 Interaction of Rep and DnaB on DNA. Nucleic Acids Res. 39: 1351–1359.

Bidnenko, V., S. D. Ehrlich, and B. Michel, 2002 Replication fork collapse at replication terminator sequences. EMBO J. 21: 3898–3907.

Bipatnath, M., P. P. Dennis, and H. Bremer, 1998 Initiation and velocity of chromosome replication in *Escherichia coli* B/r and K-12. J. Bacteriol. 180: 265–273.

Bird, R. E., J. Louarn, J. Martuscelli, and L. Caro, 1972 Origin and sequence of chromosome replication in *Escherichia coli*. J. Mol. Biol. 70: 549–566.

Bolger, A. M., M. Lohse, and B. Usadel, 2014 Trimmomatic: a flexible trimmer for Illumina sequence data. Bioinformatics 30: 2114–2120.

Bremer, H., and P. P. Dennis, 1996 Modulation of chemical composition and other parameters of the cell by growth rate, pp. 1553–1569 in *Escherichia coli and Salmonella*, edited by F. C. Neidhardt. ASM Press, Washington, DC.

Chandler, M., R. E. Bird, and L. Caro, 1975 The replication time of the *Escherichia coli* K12 chromosome as a function of cell doubling time. J. Mol. Biol. 94: 127–132.

Collier, J., 2012 Regulation of chromosomal replication in *Caulobacter crescentus*. Plasmid 67: 76–87.

Cooper, S., and C. E. Helmstetter, 1968 Chromosome replication and the division cycle of *Escherichia coli* B/r. J. Mol. Biol. 31: 519–540.

Courcelle, J., A. Khodursky, B. Peter, P. O. Brown, and P. C. Hanawalt, 2001 Comparative gene expression profiles following UV exposure in wild-type and SOS-deficient *Escherichia coli*. Genetics 158: 41–64.

Datsenko, K. A., and B. L. Wanner, 2000 One-step inactivation of chromosomal genes in *Escherichia coli* K-12 using PCR products. Proc. Natl. Acad. Sci. USA 97: 6640–6645.

Diffley, J. F., 2011 Quality control in the initiation of eukaryotic DNA replication. Philos. Trans. R. Soc. Lond. B Biol. Sci. 366: 3545–3553.

Duggin, I. G., R. G. Wake, S. D. Bell, and T. M. Hill, 2008 The replication fork trap and termination of chromosome replication. Mol. Microbiol. 70: 1323–1333.

Espéli, O., and F. Boccard, 2006 Organization of the *Escherichia coli* chromosome into macrodomains and its possible functional implications. J. Struct. Biol. 156: 304–310.

Gil, D., and J.-P. Bouché, 1991 ColE1-type vectors with fully repressible replication. Gene 105: 17–22.

Hastings, P. J., J. R. Lupski, S. M. Rosenberg, and G. Ira, 2009 Mechanisms of change in gene copy number. Nat. Rev. Genet. 10: 551–564.

Hook, S. S., J. J. Lin, and A. Dutta, 2007 Mechanisms to control rereplication and implications for cancer. Curr. Opin. Cell Biol. 19: 663–671.

Iliakis, G., 1991 The role of DNA double-strand breaks in ionising radiation-induced killing of eukaryotic cells. BioEssays 13: 641–648.

Itsko, M., and R. M. Schaaper, 2014 dGTP starvation in *Escherichia coli* provides new insights into the thymineless-death phenomenon. PLoS Genet. 10: e1004310.

Kaasch, M., and J. Kaasch, and A. Quiñones, 1989 Expression of *dnaN* and *dnaQ* genes of *Escherichia coli* is inducible by mitomycin C. Mol. Gen. Genet. 219: 187–192.

Kadaja, M., H. Isok-Paas, T. Laos, E. Ustav, and M. Ustav, 2009 Mechanism of genomic instability in cells infected with the high-risk human papillomaviruses. PLoS Pathog. 5: e1000397.

Khan, S. R., and A. Kuzminov, 2012 Replication forks stalled at ultraviolet lesions are rescued via RecA and RuvABC protein-catalyzed disintegration in *Escherichia coli*. J. Biol. Chem. 287: 6250–6265.

Khan, S. R., and A. Kuzminov, 2013 Trapping and breaking of in vivo nicked DNA during pulsed field gel electrophoresis. Anal. Biochem. 443: 269–281.

Kleinsteuber, S., and A. Quiñones, 1995 Expression of the *dnaB* gene of *Escherichia coli* is inducible by replication-blocking DNA damage in a *recA*-independent manner. Mol. Gen. Genet. 248: 695–702.

Kogoma, T., 1997 Stable DNA replication: interplay between DNA replication, homologous recombination, and transcription. Microbiol. Mol. Biol. Rev. 61: 212–238.

Kouzminova, E. A., and A. Kuzminov, 2006 Fragmentation of replicating chromosomes triggered by uracil in DNA. J. Mol. Biol. 355: 20–33.

Kouzminova, E. A., and A. Kuzminov, 2012 Chromosome demise in the wake of ligase-deficient replication. Mol. Microbiol. 84: 1079–1096.

Kouzminova, E. A., E. Rotman, L. Macomber, J. Zhang, and A. Kuzminov, 2004 RecA-dependent mutants in *E. coli* reveal strategies to avoid replication fork failure. Proc. Natl. Acad. Sci. USA 101: 16262–16267.

Kuong, K. J., and A. Kuzminov, 2009 Cyanide, peroxide and nitric oxide formation in solutions of hydroxyurea causes cellular toxicity and may contribute to its therapeutic potency. J. Mol. Biol. 390: 845–862.

Kuong, K. J., and A. Kuzminov, 2012 Disintegration of nascent replication bubbles during thymine starvation triggers RecA- and RecBCD-dependent replication origin destruction. J. Biol. Chem. 287: 23958–23970.

Kushner, S. R., 1974 In vivo studies of temperature-sensitive *recB* and *recC* mutants. J. Bacteriol. 120: 1213–1218.

Kuzminov, A., 1999 Recombinational repair of DNA damage in *Escherichia coli* and bacteriophage l. Microbiol. Mol. Biol. Rev. 63: 751–813.

Kuzminov, A., 2011 Homologous recombination: experimental systems, analysis, and significance, chap. 7.2.6 in *EcoSal: Escherichia coli and Salmonella: Cellular and Molecular Biology*, edited by A. Böck, R. Curtiss III, J. B. Kaper, P. D. Karp, and F. C. Neidhardt *et al*. ASM Press, Washington, DC.

Kuzminov, A., 2013 The chromosome cycle of prokaryotes. Mol. Microbiol. 90: 214–227.

Kuzminov, A., 2014 The precarious prokaryotic chromosome. J. Bacteriol. 196: 1793–1806.

Lane, H. E. D., and D. T. Denhardt, 1975 The *rep* mutation. IV. Slower movement of the replication forks in *Escherichia coli rep* strains. J. Mol. Biol. 97: 99–112.

Leonard, A. C., and M. Méchali, 2013 DNA replication origins. Cold Spring Harb. Perspect. Biol. 5: a010116.

Li, H., and R. Durbin, 2009 Fast and accurate short read alignment with Burrows-Wheeler transform. Bioinformatics 25: 1754–1760.

Li, H., B. Handsaker, A. Wysoker, T. Fennell, J. Ruan *et al.*, 2009 1000 Genome Project Data Processing Subgroup. The Sequence Alignment/Map format and SAMtools. Bioinformatics 25: 2078–2079.

Liang, C., J. D. Spitzer, H. S. Smith, and S. A. Gerbi, 1993 Replication initiates at a confined region during DNA amplification in Sciara DNA puff II/9A. Genes Dev. 7: 1072–1084.

Mahaseth, T., and A. Kuzminov, 2015 Cyanide enhances hydrogen peroxide toxicity by recruiting endogenous iron to trigger catastrophic chromosomal fragmentation. Mol. Microbiol. 96: 349–367.

Martín, C. M., and E. C. Guzmán, 2011 DNA replication initiation as a key element in thymineless death. DNA Repair (Amst.) 10: 94–101.

Masai, H., S. Matsumoto, Z. You, N. Yoshizawa-Sugata, and M. Oda, 2010 Eukaryotic chromosome DNA replication: where, when, and how? Annu. Rev. Biochem. 79: 89–130.

Michel, B., S. D. Ehrlich, and M. Uzest, 1997 DNA double-strand breaks caused by replication arrest. EMBO J. 16: 430–438.

Miller, J. H., 1972 *Experiments in Molecular Genetics*. Cold Spring Harbor Laboratory Press, Cold Spring Harbor, NY.

Miranda, A., and A. Kuzminov, 2003 Chromosomal lesion suppression and removal in *Escherichia coli* via linear DNA degradation. Genetics 163: 1255–1271.

Mirkin, E. V., and S. M. Mirkin, 2007 Replication fork stalling at natural impediments. Microbiol. Mol. Biol. Rev. 71: 13–35.

Mohana-Borges, R., A. B. Pacheco, F. J. Sousa, D. Foguel, D. F. Almeida *et al.*, 2000 LexA repressor forms stable dimers in solution. The role of specific DNA in tightening protein-protein interactions. J. Biol. Chem. 275: 4708–4712.

Morigen, I. O., and K. Skarstad, 2009 Growth rate dependent numbers of SeqA structures organize the multiple replication forks in rapidly growing *Escherichia coli*. Genes Cells 14: 643–657.

Murray, H., and J. Errington, 2008 Dynamic control of the DNA replication initiation protein DnaA by Soj/ParA. Cell 135: 74–84.

Nielsen, H. J., B. Youngren, F. G. Hansen, and S. Austin, 2007 Dynamics of Escherichia coli chromosome segregation during multifork replication. J. Bacteriol. 189: 8660–8666.

Olsson, J., S. Dasgupta, O. G. Berg, and K. Nordström, 2002 Eclipse period without sequestration in *Escherichia coli*. Mol. Microbiol. 44: 1429–1440.

Olsson, J. A., K. Nordström, K. Hjort, and S. Dasgupta, 2003 Eclipse-synchrony relationship in *Escherichia coli* strains with mutations affecting sequestration, initiation of replication and superhelicity of the bacterial chromosome. J. Mol. Biol. 334: 919–931.

Petes, T. D., and D. H. Williamson, 1994 A novel structural form of the 2 micron plasmid of the yeast *Saccharomyces cerevisiae*. Yeast 10: 1341–1345.

Quinlan, A. R., and I. M. Hall, 2010 BEDTools: a flexible suite of utilities for comparing genomic features. Bioinformatics 26: 841–842.

Quinn, W. G., and N. Sueoka, 1970 Symmetric replication of the *Bacillus subtilis* chromosome. Proc. Natl. Acad. Sci. USA 67: 717–723.

Resnick, M. A., 1978 Similar responses to ionizing radiation of fungal and vertebrate cells and the importance of DNA double-strand breaks. J. Theor. Biol. 71: 339–346.

Rotman, E., P. Bratcher, and A. Kuzminov, 2009 Reduced lipopolysaccharide phosphorylation in *Escherichia coli* lowers the elevated ori/ter ratio in *seqA* mutants. Mol. Microbiol. 72: 1273–1292.

Rotman, E., S. R. Khan, E. Kouzminova, and A. Kuzminov, 2014 Replication fork inhibition in *seqA* mutants of *Escherichia coli* triggers replication fork breakage. Mol. Microbiol. 93: 50–64.

Russo, F. D., I. Scherson, and J. R. Broach, 1992 Direct simulation of yeast 2-microns circle plasmid amplification. J. Theor. Biol. 155: 369–385.

Salguero, I., E. L. Acedo, and E. C. Guzmán, 2011 Overlap of replication rounds disturbs the progression of replicating forks in a ribonucleotide reductase mutant of *Escherichia coli*. Microbiology 157: 1955–1967.

Sangurdekar, D. P., B. L. Hamann, D. Smirnov, F. Srienc, P. C. Hanawalt *et al.*, 2010 Thymineless death is associated with loss of essential genetic information from the replication origin. Mol. Microbiol. 75: 1455–1467.

Sernova, N. V., and M. S. Gelfand, 2008 Identification of replication origins in prokaryotic genomes. Brief. Bioinform. 9: 376–391.

Sinha, N. K., and D. P. Snustad, 1972 Mechanism of inhibition of deoxyribonucleic acid synthesis in *Escherichia coli* by hydroxyurea. J. Bacteriol. 112: 1321–1334.

Skarstad, K., and T. Katayama, 2013 Regulating DNA replication in bacteria. Cold Spring Harb. Perspect. Biol. 5: a012922.

Smith, G. R., 2012 How RecBCD enzyme and Chi promote DNA break repair and recombination: a molecular biologist's view. Microbiol. Mol. Biol. Rev. 76: 217–228.

Spradling, A. C., 1981 The organization and amplification of two chromosomal domains containing *Drosophila* chorion genes. Cell 27: 193–201.

Stokke, C., T. Waldminghaus, and K. Skarstad, 2011 Replication patterns and organization of replication forks in *Vibrio cholerae*. Microbiology 157: 695–708.

Sutera, V. A. J., and S. T. Lovett, 2006 The role of replication initiation control in promoting survival of replication fork damage. Mol. Microbiol. 60: 229–239.

Syu, L. J., and M. M. Fluck, 1997 Site-specific in situ amplification of the integrated polyomavirus genome: a case for a context-specific over-replication model of gene amplification. J. Mol. Biol. 271: 76–99.

Truong, L. N., Y. Li, E. Sun, K. Ang, P. Y. Hwang *et al.*, 2014 Homologous recombination is a primary pathway to repair DNA double-strand breaks generated during DNA rereplication. J. Biol. Chem. 289: 28910–28923.

Uzest, M., S. D. Ehrlich, and B. Michel, 1995 Lethality of *rep recB* and *rep recC* double mutants of *Escherichia coli*. Mol. Microbiol. 17: 1177–1188.

Vallet-Gely, I., and F. Boccard, 2013 Chromosomal organization and segregation in *Pseudomonas aeruginosa*. PLoS Genet. 9: e1003492.

Viollier, P. H., M. Thanbichler, P. T. McGrath, L. West, M. Meewan *et al.*, 2004 Rapid and sequential movement of individual chromosomal loci to specific subcellular locations during bacterial DNA replication. Proc. Natl. Acad. Sci. USA 101: 9257–9262.

von Freiesleben, U., M. A. Krekling, F. G. Hansen, and A. Løbner-Olesen, 2000 The eclipse period of *Escherichia coli*. EMBO J. 19: 6240–6248.

Waldminghaus, T., and K. Skarstad, 2009 The *Escherichia coli* SeqA protein. Plasmid 61: 141–150.

Wang, J. D., M. B. Berkmen, and A. D. Grossman, 2007 Genome-wide coorientation of replication and transcription reduces adverse effects on replication in *Bacillus subtilis*. Proc. Natl. Acad. Sci. USA 104: 5608–5613.

Zaritsky, A., C. L. Woldringh, M. Einav, and S. Alexeeva, 2006 Use of thymine limitation and thymine starvation to study bacterial physiology and cytology. J. Bacteriol. 188: 1667–1679.

Zaritsky, A., N. Vischer, and A. Rabinovitch, 2007 Changes of initiation mass and cell dimensions by the 'eclipse.' Mol. Microbiol. 63: 15–21.

Zhang, F., W. Gu, M. E. Hurles, and J. R. Lupski, 2009 Copy number variation in human health, disease, and evolution. Annu. Rev. Genomics Hum. Genet. 10: 451–481.

Communicating editor: S. J. Sandler

GENETICS

Supporting Information
www.genetics.org/lookup/suppl/doi:10.1534/genetics.115.184697/-/DC1

Static and Dynamic Factors Limit Chromosomal Replication Complexity in *Escherichia coli*, Avoiding Dangers of Runaway Overreplication

Sharik R. Khan, Tulip Mahaseth, Elena A. Kouzminova, Glen E. Cronan, and Andrei Kuzminov

DOI: 10.1534/genetics.115.184697

Supplement to the MS by

Sharik R. Khan, Tulip Mahaseth, Elena A. Kouzminova, Glen Cronan and Andrei Kuzminov

Static and dynamic factors limit chromosomal replication complexity in *Escherichia coli*, avoiding dangers of runaway overreplication

Table S1. Strains and plasmids used in this study.

Strain	**Relevant genotype***	**Reference**
Published		
AB1157	Wild-type strain*	(*1*)
ER16	Δ*seqA21*	(*2*)
JJC213	Δ*rep*::*kan*	*(3)*
SK129	*recB270*(Ts) *recC271*(Ts)	(*4*)
SRK325	SK129 with chromosome::pSRK-ori2 (Amp^R)	(*5*)

This study	Derivation / relevant genotype	Drug resistance
1157-IOC	AB1157 with chromosome::pSRK-ori2	Amp^R
SRK252	SRK325 with one copy of *kup* replaced (Δ*kup::kan*)	Amp^R Km^R
SRK253	1157-IOC Δ*kup::kan*	Amp^R Km^R
SRK253-1	SRK253 *recA938::cat*	Amp^R Km^R Cm^R
SRK253-1/2	SRK253 *recA306::Tn10*	Amp^R Km^R Tet^R
SRK253-2	SRK253 *ΔruvABC1::cat*	Amp^R Km^R Cm^R
SRK253-2/1.1	SRK253 *ΔruvABC1::cat*	Amp^R Cm^R
SRK253-3	SRK253 *ΔrecD1903::tet*	Amp^R Km^R Tet^R
SRK253-4	AB1157 *ΔseqA21*-EOC Δ*kup::kan*	Amp^R Km^R
SRK253-5	SRK253 *Δrep::cat*	Amp^R Km^R Cm^R

SRK253-6	SRK253 *ΔrecF::cat*	Amp^R Km^R Cm^R
SRK253-7	SRK253 *ΔruvABC1::cat recG258::kan*	Amp^R Km^R Cm^R
SRK253-8/2	SRK253 *ΔruvABC1::cat recA306::Tn10*	Amp^R Km^R Tet^R
SRK253-9	SRK253 *recC266::Tn10*	Amp^R Km^R Tet^R
SRK253-13	SRK253 *lexA3*(*malB::Tn10*)	Amp^R Km^R Tet^R
TM11	Δ*seqA21* Δ*rep*::*kan*	Km^R

* — complete genotype of AB1157 includes: F– λ– rac- *thi-1 hisG4 Δ(gpt-proA)62 argE3 thr-1 leuB6 kdgK51 rfbD1 araC14 lacY1 galK2 xylA5 mtl-1 tsx-33 glnV44 rpsL31*

Table S2. The numbers of replication bubbles behind replication complexity indices (ori/ter ratios) illustrate the concept of "replication fork crowding".

Ori/ter ratio	# of replication bubbles per chromosome
1	0
2	1
4	3
8	7
16	15
32	31
64	63

Supplemental figures with legends

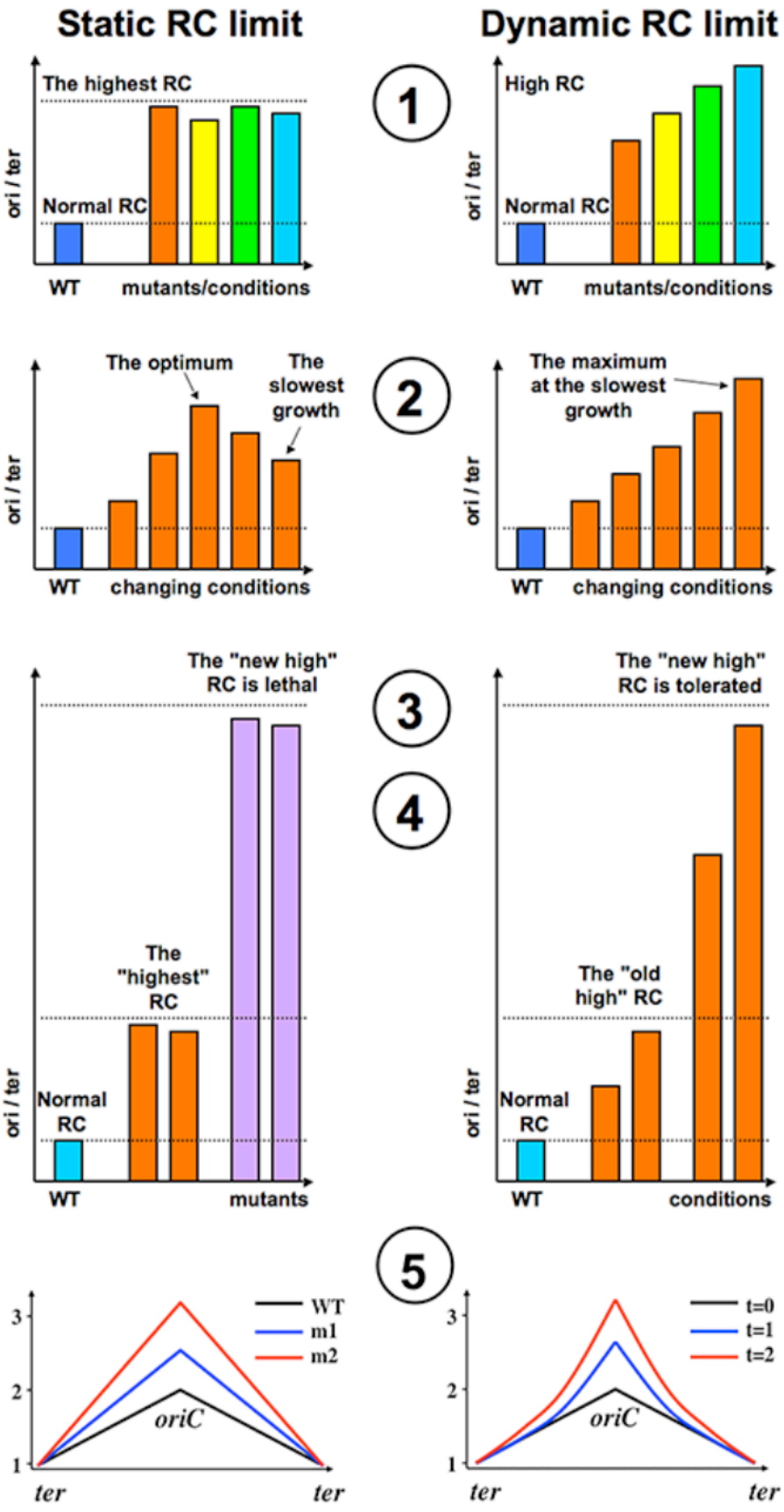

Figure S1. A schematic presentation of imaginary experimental results consistent with either the static or the dynamic nature of replication complexity regulation. Explanations are in the text.

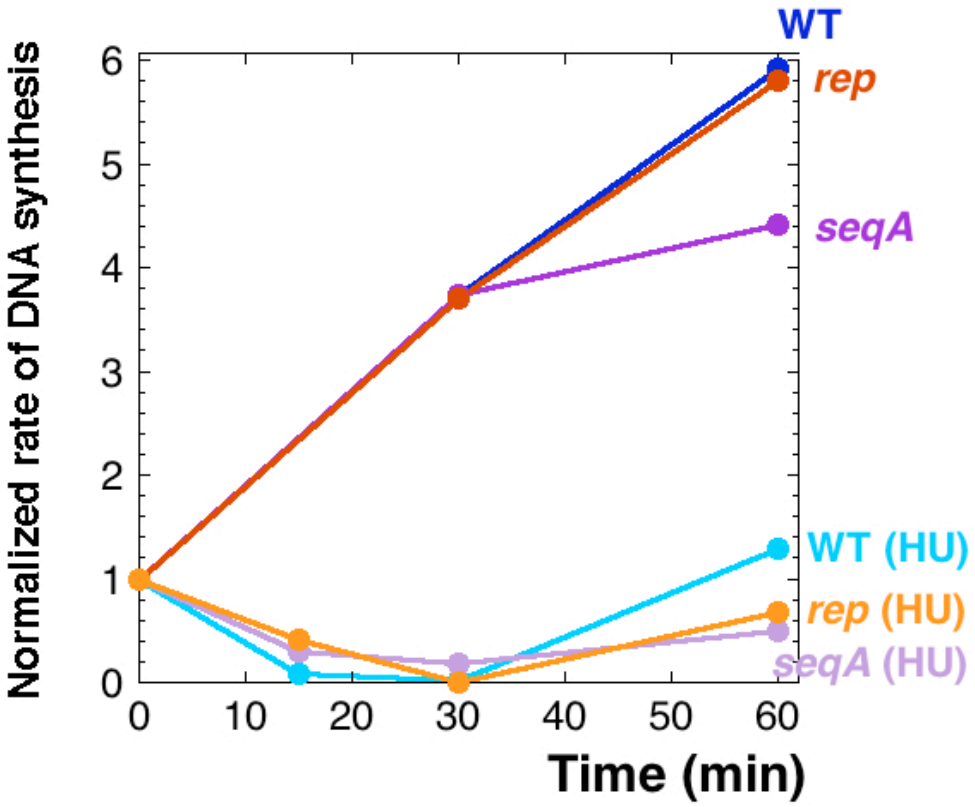

Figure S2. The rate of DNA synthesis upon inhibition with 10 mM HU. Uninhibited cultures are shown as controls. The rates were measured by incorporation of ^{3}H Thymidine into acid-insoluble material and normalized to those at time 0 minutes.

Protocol:

Overnight cultures were diluted 100-fold, grown to an OD=0.2 in LB at 28°C, split in two, and one half was supplemented with 10 mM HU (time 0). At the indicated time points, 200 µl aliquots of the cultures were incubated with 200 µl of M9 minimal medium supplemented with 40 µg/ml of *arginine*, *histidine*, *proline*, leucine and threonine, 1µCi/ml of ^{3}H Thymidine and 2 µg/ml of cold thymidine, for 5 minutes at room temperature. After precipitation with 5 ml ice-cold 5% trichloroacetic acid (TCA), filtering through GF/A filters and wash with 5 ml of 5% TCA, followed by 5 ml ethanol and drying, the counts on the filters were measured in a liquid scintillation counter. As a background, the lowest count of the set was used. This unusual manipulation was done this time because our standard DNA incorporation background — *E. coli* cells killed with 200 J/m^{2} UV, — incorporated a little bit more than our lowest HU-inhibited culture did. This is why we decided to "zero" that particular value, instead of presenting a negative value.

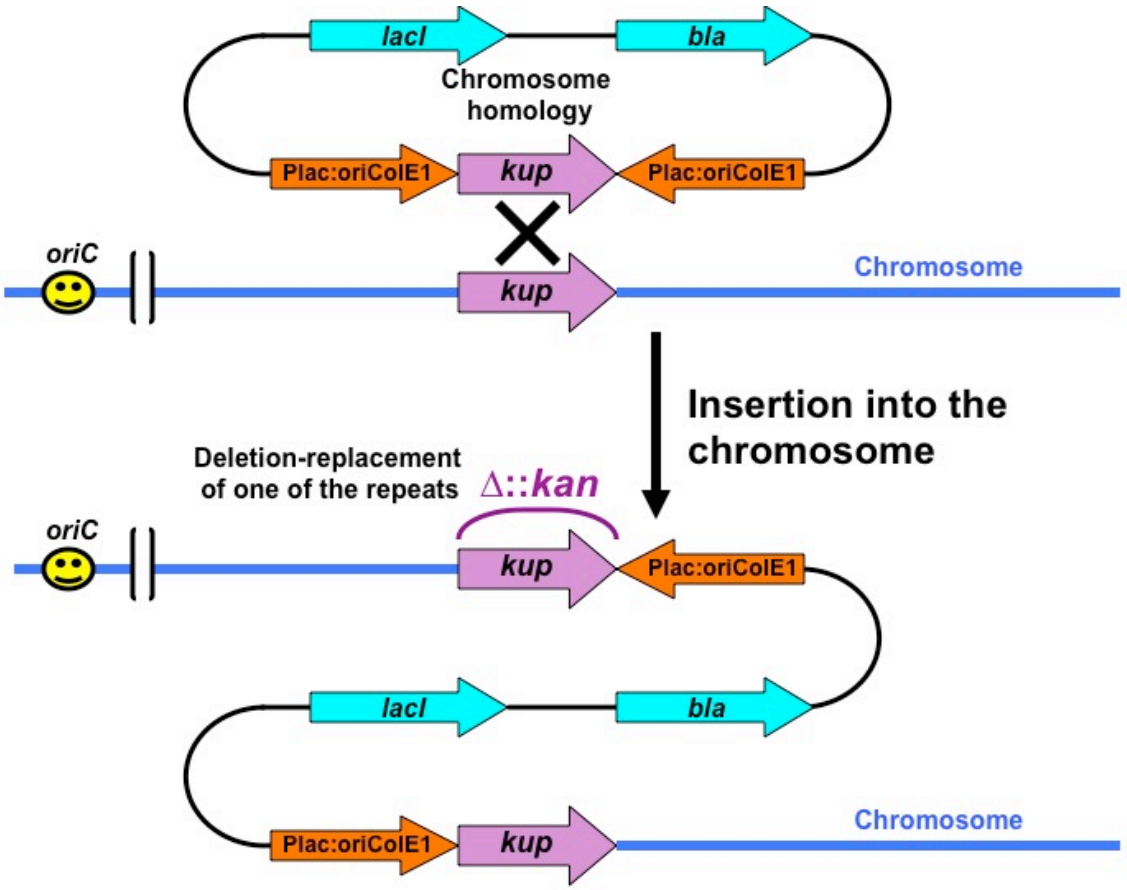

Figure S3. A scheme of inducible origin construct (IOC). The integrating plasmid was pSRK-ori2. The chromosome homology was at the *kup* locus.

The IPTG-controlled replication origin was constructed by Gil and Bouche (*6*), who fused the RNAII transcript of the pBR322 replication origin with the *lacZ* promoter-operator region, reversing the whole origin relative to the upstream *bla* gene to prevent read-through, and providing the *lacI*^{q} gene on the same plasmid. Like the original ColE1 origin of pBR322, this origin is regulated positively by expression of RNAII and negatively by antisense expression of RNAI from a strong constitutive promoter.

Stable replication of such plasmid requires 1 mM IPTG, while the copy number of the IPTG-dependent replicon is at least 10 (*6*) (but likely higher). Due to its moderate copy number, the plasmid could still function (although rather poorly) as an insertional suppressor into a chromosome of the *dnaA* mutants (*6*). The steady-state copy number of this origin in the chromosome has not been measured before.

Our previous experience with this IPTG-driven origin inserted into the chromosome (*7*) shows that a single replication origin is still partially unidirectional (the original ColE1 origin is considered to be unidirectional). Therefore, for this project we assembled its inverted duplication, to make replication gradients in both directions symmetrical.

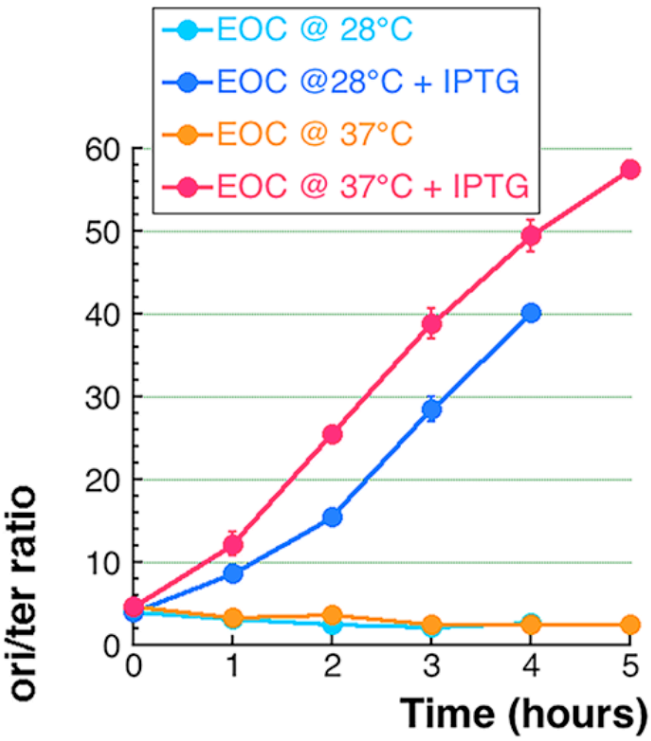

Figure S4. Kinetics of the ori/ter ratio upon IPTG induction in the SRK253 strain at 28°C versus 37°C. The missing error bars (SEM) are actually masked by the symbols.

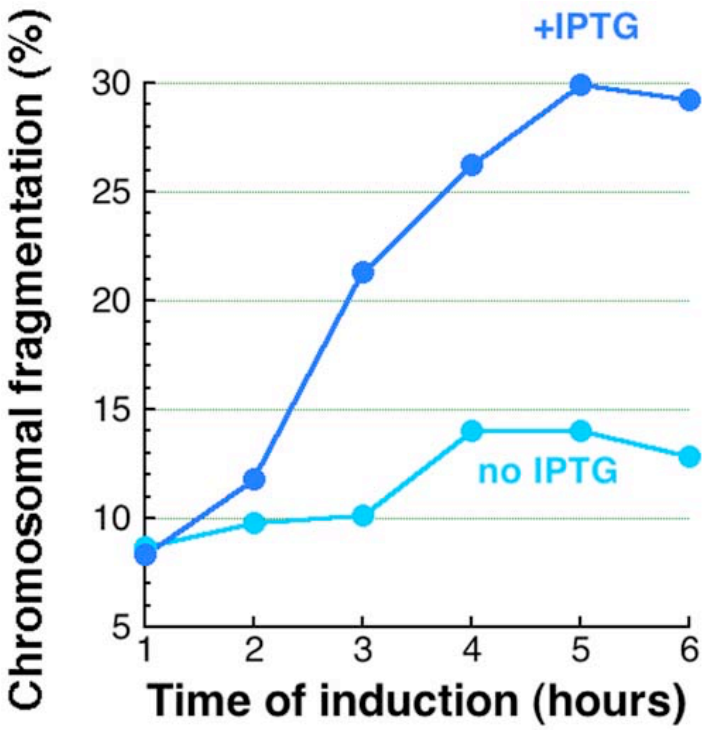

Figure S5. Kinetics of chromosome fragmentation as a result of induced overreplication. The strain is SRK252 (IOC *recBC*(Ts)).

Supplemental references

1. B. J. Bachmann, in *Escherichia coli and Salmonella typhimurium. Cellular and Molecular Biology,* F. C. Neidhardt, Ed. (American Society for Microbiology, Washington, D.C., 1987), pp. 1190-1219.
2. E. Rotman, A. Kuzminov, The *mutT* defect does not elevate chromosomal fragmentation in *Escherichia coli* because of the surprisingly low levels of MutM/MutY-recognized DNA modifications. *J. Bacteriol.* **189**, 6976-6988 (2007).
3. M. Uzest, S. D. Ehrlich, B. Michel, Lethality of *rep recB* and *rep recC* double mutants of *Escherichia coli*. *Mol. Microbiol.* **17**, 1177-1188 (1995).
4. S. R. Kushner, In vivo studies of temperature-sensitive *recB* and *recC* mutants. *J. Bacteriol.* **120**, 1213-1218 (1974).
5. E. Rotman, S. R. Khan, E. Kouzminova, A. Kuzminov, Replication fork inhibition in *seqA* mutants of *Escherichia coli* triggers replication fork breakage. *Mol. Microbiol.* **93**, 50-64 (2014).
6. D. Gil, J.-P. Bouché, ColE1-type vectors with fully repressible replication. *Gene* **105**, 17-22 (1991).
7. E. A. Kouzminova, A. Kuzminov, Patterns of chromosomal fragmentation due to uracil-DNA incorporation reveal a novel mechanism of replication-dependent double-strand breaks. *Mol. Microbiol.* **68**, 202-215 (2008).